JCI insight

Immunization using ApoB-100 peptide-linked nanoparticles reduces atherosclerosis

Kuang-Yuh Chyu, … , Eun Ji Chung, Prediman K. Shah

JCI Insight. 2022. https://doi.org/10.1172/jci.insight.149741.

Research In-Press Preview Cardiology Vaccines

Graphical abstract

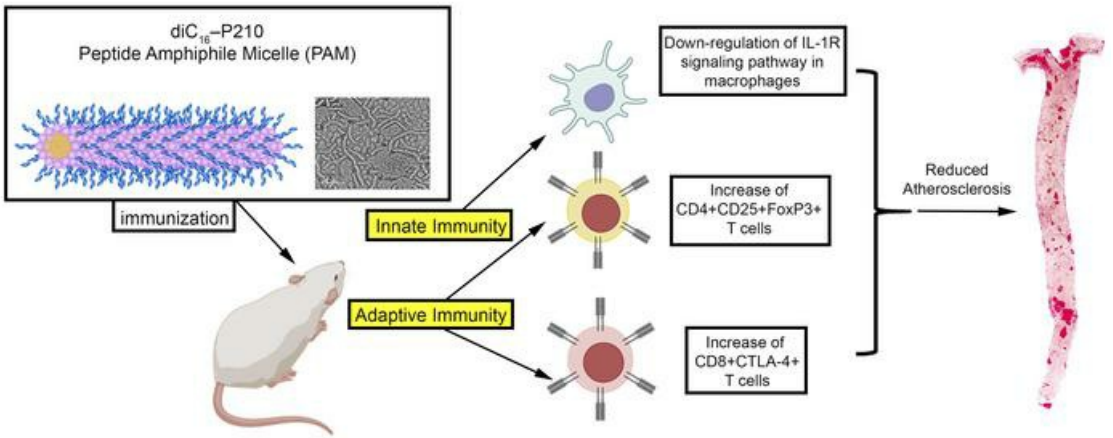

Immunization using ApoB-100 peptide-linked nanoparticles reduces atherosclerosis

Kuang-Yuh Chyu, MD, PhD,[1] Xiaoning Zhao, PhD,[1] Jianchang Zhou, PhD,[1] Paul C Dimayuga, PhD,[1] Nicole WM Lio, BS,[1] Bojan Cercek, MD,[1] Noah Trac, BS,[2] Eun Ji Chung, PhD,[2] Prediman K Shah, MD.[1]

[1]Oppenheimer Atherosclerosis Research Center, Department of Cardiology, Smidt Heart Institute, Cedars-Sinai Medical Center, Los Angeles, California, U.S.A.

[2]Department of Biomedical Engineering, University of Southern California, Los Angeles, California, U.S.A.

Correspondence

Kuang-Yuh Chyu, MD, PhD

Department of Cardiology

Smidt Heart Institute

Cedars-Sinai Medical Center

127 S San Vincente Blvd, Suite A3311B

Los Angeles, CA 90048

(310) 423-8580

Chyuk@cshs.org

Conflict of interest

PKS and KYC are coinventors of ApoB-100 peptide vaccines and have assigned patent rights to Cedars-Sinai Medical Center. PKS is an unpaid member of the Board of Directors for Abcentra Inc.

Abstract

We have previously demonstrated that active immunization with the apolipoprotein B-100 (ApoB-100) peptide P210 reduces experimental atherosclerosis. To advance this immunization strategy to future clinical testing, we explored the possibility of delivering P210 as an antigen using nanoparticles, given this approach has now been used clinically. To that end, we first charactered the responses of T cells to P210 using PBMCs from human subjects with atherosclerotic cardiovascular disease (ASCVD). We then investigated the use of P210 in self-assembling peptide amphiphile micelles (P210-PAM) as a vaccine formulation to reduce atherosclerosis in *ApoE*$^{-/-}$ mice and its potential mechanisms of action. We also generated and characterized a humanized mouse model with chimeric *HLA-A*02:01/Kb* in *ApoE*$^{-/-}$ background to test the efficacy of P210-PAM immunization as a bridge for future clinical testing.

P210 provoked T cell activation and memory response in PBMCs of human subjects with ASCVD. Dendritic cell uptake of P210-PAM and its co-staining with MHC-I molecules supported its use as a vaccine formulation. In *ApoE*$^{-/-}$ mice, immunization with P210-PAM dampened P210-specific CD4+ T cell proliferative response and CD8+ T cell cytolytic response, modulated macrophage phenotype, and significantly reduced aortic atherosclerosis. Potential clinical relevance of P210-PAM immunization was demonstrated by reduced atherosclerosis in the humanized *ApoE*$^{-/-}$ mouse model expressing chimeric *HLA-A*02:01/Kb*. Taken together, our data supports the experimental and translational use of P210-PAM as a potential vaccine candidate against human ASCVD.

Introduction

Adaptive immune responses against self-antigens such as LDL, ApoB-100 or certain ApoB-100 related peptide epitopes is a hallmark of experimental and human atherosclerosis (1-3). Among the ApoB-100 peptides, P210 is the subject of several investigations to develop antigen-specific immune modulation (4-7). We have previously demonstrated P210-specific CD8+ T cells in hypercholesterolemic mice can be detected by peptide-loaded synthetic soluble MHC-I pentamers. These P210-specific CD8+ T cells increased in response to atherogenic diet, correlated with the extent of atherosclerosis, and localized to atherosclerotic plaques (8). Additionally, P210 fragments and P210-specific antibodies have been detected in plaques and circulation of patients with atherosclerotic cardiovascular disease (ASCVD), suggesting the involvement of P210 in human atherosclerotic disease (9;10).

An outcome of various experimental strategies of P210 immune modulation is alteration of T cell responses to P210 suggesting that the peptide or derivatives thereof are self-antigens that provoke immune responses involved in atherosclerosis (5;11). We have demonstrated that P210, when used in an active immunization strategy, elicited CD8+ T cell response to reduce atherosclerosis (4), potentially by shifting the immune-dominant epitope (8). These experimental observations implicate immune response to P210 in atherogenesis and suggest that modification of the intrinsic immune response to P210 could potentially reduce human atherosclerosis.

In preclinical studies, immunogenic peptides are often conjugated as haptens to carrier molecules along with an adjuvant such as mineral salt to provoke an immune response to establish vaccine efficacy. Traditional aluminum salt based vaccines are known to induce weak

cell-mediated immune responses, limiting their clinical application and choice of antigens (12;13). The evidence from work with P210 immunization in animal models shows the involvement of various cellular immune responses such as regulatory T cell or CD8+ T cell responses (4;5;11;14). We therefore surmised that an approach targeting immune regulation of the response to P210 would be beneficial in atherosclerosis. One effective way to deliver antigens that provoke a regulatory response is to use the nanoparticle platform (15).

Mechanistically, nanoparticles have favorable physicochemical properties that provide size-preferential lymphatic transport, relatively long injection-site retention and circulating time for contact with dendritic cells, acting as adjuvants in subunit vaccines, and the induction of auto-immunity specific regulatory immune responses (16). A variety of nanoparticle platforms have been tested to target inflammation and to modulate immune function in atherosclerosis with wide potential in humans (17-21). More importantly, nanoparticle based vaccines are already in clinical use to prevent COVID-19 infection and being tested in a clinical trial to treat autoimmune disease such as celiac disease (22).

In this study, we first assessed the clinical relevance of P210 as a self-antigen in ASCVD by demonstrating that P210 provokes T cell responses in patients with acute coronary syndrome. We then utilized the peptide amphiphile nanoparticle platform in which the P210 is chemically conjugated to hydrophobic tails, facilitating subsequent self-assembly into well-defined peptide amphiphile micelles (PAMs) (23-25). PAMs were used as nanocarriers because they are comprised of biocompatible lipids and peptides and are chemically versatile, allowing the incorporation of multiple modalities such as fluorescence and immunogenicity into a single particle. We tested if the PAM nanoparticle platform can function as a novel vaccine

formulation to reduce atherosclerosis in hypercholesterolemic *ApoE*$^{-/-}$ mice and explored its potential mechanisms of achieving such effect. As a bridge to potential human testing, we developed a chimeric *HLA-A*02:01/Kb ApoE*$^{-/-}$ humanized mouse model (*A2Kb Tg ApoE*$^{-/-}$ mice) to test the efficacy of P210-PAM. The focus on Class-I HLA-A*02:01 is supported by our previous report demonstrating the importance of the Class-I MHC/CD8+ T cell pathway in both the intrinsic immune response to P210 as well as potential immune-modulating therapy (4;8). Herein, we report the effects of P210-PAM immunization on immune responses in atherosclerosis and tested the translational application of the P210-PAM formulation as a potential human vaccine using *A2Kb Tg ApoE*$^{-/-}$ mice.

Results

Intrinsic T cell response to ApoB-100 peptide P210 in ACS patients

We previously demonstrated that immune modulation of T cells reactive with the ApoB-100 peptide P210 in *ApoE*$^{-/-}$ mice reduced atherosclerosis (4). To evaluate if self-reactive T cell response to P210 is present in humans, we investigated the intrinsic T cell response to P210 in humans by testing peripheral blood mononuclear cells (PBMCs) from acute coronary syndrome (ACS) patients and self-reported healthy volunteers as controls. ACS patients were selected for this exploratory study because of unequivocal ASCVD in these subjects. Patient characteristics are in Table 1.

In order to determine if P210 is capable of activating T cells as an antigen, we conducted an Activation Induced Marker (AIM) assay (26-28). At baseline, there were lower CD4+CD69+ T cells and higher CD8+CD25+ T cells in PBMCs from ACS patients compared to control subjects, whereas no difference in CD4+CD25+ and CD8+CD69+ T cells between 2 groups were noted (Figure 1A-1D, P=0.07 for Figure 1B, P=0.05 for Figure 1C). AIM assays demonstrated a mean 1.5-fold increase in CD4+CD69+CD134+ T cells after P210 stimulation in ACS patients compared to control subjects while no such increase was observed in CD8+CD69+CD134+ T cells (Figure 1E, 1F). CMV pooled peptide (right panel in Figure 1E, 1F) or cell stimulation cocktail (PMA/Ionomycin, Supplementary Figure 1A-1F) as positive controls validated the AIM assay. We did not observe differences in CD25+CD134+, CD69+CD154+ or CD134+CD137+ in either CD4+ or CD8+ T cells (Supplementary Figure 1G-1L). Although a cut-off of 2-fold increase may be appropriate in studying T cell activation to exogenous antigens (infectious or vaccine antigens), T cell responses to intrinsic self-antigens are not expected to be as robust, since the

immune-inflammatory response to self-antigens in auto-immune diseases tend to be chronic and low grade.

A hallmark feature of adaptive immune response is the recall response of antigen-experienced T cells to antigen re-exposure. Given ACS patients have definite atherosclerosis, we tested if T cells from ACS patients would generate such recall response to P210 restimulation. CD4+ T Effector cell response to P210 was not significantly different in the ACS PBMCs compared to controls (Figure 1G & H). However, there was a significant increase in CD8+ T Effector (Figure 1I), and CD8+ T Effector Memory (Figure 1J; gating strategy for T cells in Figure 1K) response in ACS PBMCs compared to controls, which supports the existence of antigen-experienced, P210-specific T cells in humans with atherosclerosis.

Characteristics of P210 peptide

The T cell response observed in PBMCs from ACS patients suggested that P210 may be a self-peptide that provokes a self-reactive immune response. It remains unknown how apolipoprotein B-100 (ApoB-100) peptides become immunogenic, but the presence of antibodies against ApoB-100 peptides in patients with ASCVD suggests the potential of antigen presenting cells (APC) to present peptides derived from LDL particles that have undergone oxidation and subsequent breakdown (9;29-31). Indeed, various ApoB-100 peptide fragments, including P210, have been detected in atherosclerotic plaques by mass spectrometry (10). However, it remains unknown how ApoB-100 peptides, specifically P210, are able to enter dendritic cells (DCs) to function as intrinsic self-antigens.

P210 is a cationic peptide fragment that is within the proteoglycan binding domain of ApoB-100 that has the properties of a cell-penetrating peptide (CPP). Cationic CPPs are rich in

positively charged Arg and Lys residues, which enable interaction with negatively charged cell surface proteoglycans (32;33). Given the Lys-rich sequence of P210 (**K**TT**K**QSFDLSV-**K**AQY**KK**N**K**H) and a calculated isoelectric point (pI) of 10.85, we investigated if P210 could enter mouse bone marrow-derived DCs through the proteoglycan pathway. We first used confocal microscopy to visualize the uptake of FITC-conjugated P210 peptides (P210-FITC) into CD11c+ DCs, and flow cytometric analysis confirmed significantly increased uptake of P210-FITC (Figure 2A-C). The proteoglycan binding capacity of P210 was assessed by using heparin to block DC uptake (34) and P210-FITC entry into DCs was significantly reduced by 100U/ml of heparin (Figure 2D). To further confirm that the cellular uptake of P210 is mediated by cell surface proteoglycan binding, DCs were treated with p-nitrophenyl-β-D-xylopyranoside (pNP-xyl), a competitive inhibitor of heparan sulfate chain addition, preventing the synthesis of functional cell surface heparan sulfate proteoglycans (35). Treatment of DCs with pNP-xyl significantly reduced P210-FITC entry (Figure 2E), supporting the notion that P210 uptake by DCs is mediated in part through cell surface proteoglycan binding. The results demonstrate that P210 has properties of a CPP that enables its entry into APCs such as DCs and potentially presented to T cells as a self-peptide.

Immune modulation and biodistribution of P210 nanoparticles

To enable efficient antigen delivery by protecting peptides from protease degradation and clearance and providing a scaffold for increased epitope density, P210 was incorporated into peptide amphiphile micelles (PAMs) through covalent conjugation of the peptide to 1'-3'-dihexadecyl *N*-succinyl-$_L$-glutamate (diC_{16}) hydrophobic moieties. Hydrophobic interaction induced self-assembly of the diC_{16}-P210 monomers into cylindrical micelles with an average

diameter of 21.6 ± 1.1 nm, a polydispersity index of 0.152 ± 0.001 and a zeta potential of 2.7 ± 0.8 mV (Figure 3A - 3C, Supplementary Figure 2 and Figure 3).

First, we tested whether P210-PAM enters DCs and if P210 (or its fragment) can be costained with MHC-I by conducting confocal experiments using FITC-labeled P210-PAM. MHC-I was chosen as the pathway to visualize given prior data indicating the involvement of MHC-I/CD8+ T cell pathway in P210 immunization, consistent with the reported characterization of CPPs to be cross-presented to MHC-I (34;36). Confocal microscopy demonstrated costaining of FITC-labelled P210 with MHC-I molecule on the surface of mouse DCs (Figure 3E-3I).

P210-PAM was then tested for reactivity with T cells of *ApoE*$^{-/-}$ mice and Mouse Serum Albumin peptide amphiphile micelles (MSA-PAM) were used as a control. There was a significant reduction in CD4+ effector memory T cells and increase in CD8+ central memory T cells treated with P210-PAM when compared to MSA-PAM treated splenocytes of *ApoE*$^{-/-}$ mice fed high cholesterol diet for 16 weeks (Figure 3K, 3L). Although central memory CD4+ T cells and effector memory CD8+ T cells remained unchanged (Figure 3J, 3M), the results suggest that P210-PAM provokes a memory T cell response in naïve hypercholesterolemic *ApoE*$^{-/-}$ mice.

Effective immunization depends not only on the immunogenicity of antigens but also on their retention at the injection site (37). We hence characterized the biodistribution kinetics of fluorescently labeled P210-PAM injected subcutaneously in wild type mice and imaged over a period of 7 days, showing 80%, 30% and 15% retention in the injection site at 2, 5 and 7 days, respectively with a calculated clearance half-life 79.7 ± 29.2 hrs (Figure 4A, 4B). Immuno-fluorescent staining of the injection site showed colocalization of P210-PAM with F4/80+ macrophages and CD11c+ DCs (Figure 4C). MSA-PAM had percent retention of 67%, 37%, and

11% at 2, 5, and 7 days, respectively, and the clearance half-life of 72.7 ± 29.2 hrs (Figure 4D - 4F).

Nanoparticle-based immune modulation of T cell responses to P210-PAM immunization

The effect of P210-PAM immunization on immune regulation was then tested in *ApoE*$^{-/-}$ mice, using the MSA-PAM as a control. Immunized male *ApoE*$^{-/-}$ mice euthanized 1 week after the second booster injection showed no differences in splenic CD4+PD1+ and CD4+CTLA-4+ T cells between P210-PAM and MSA-PAM immunized mice (Figure 5A, 5B). There was increased CD4+CD25+FoxP3+ T_{reg} cells in P210-PAM immunized mice compared to those immunized with MSA-PAM (Figure 5C, *P*=0.05). There were no differences in CD8+PD1+ T cell numbers (Figure 5D) but CD8+CTLA-4+ T cells were significantly increased in P210-PAM immunized mice compared to MSA-PAM immunized mice (Figure 5E). CD4+ T cells from P210-PAM immunized mice had significantly reduced proliferative response to P210 stimulation compared to CD4+ T cells from MSA-PAM immunized mice (Figure 5F) but this was not observed in CD8+ T cells (Figure 5G). CD4+ T cells (Figure 5H) and CD8+ T cells (Figure 5I) responded to Con A stimulation similarly between the 2 groups suggesting specificity of the regulation of T cell response. Even though P210-PAM immunization had no effect on CD8+ T cells proliferation, there was reduced cytolytic function of CD8+ T cells in response to P210 stimulation in P210-PAM immuized mice compared to MSA-PAM immunized mice as determined by CD107a staining (Figure 5J). Thus, P210-PAM provoked antigen-specific effects as well as regulation of CD4+ T cells proliferation and CD8+ T cells cytolytic function. No differences were observed in dendritic cell phenotypes (Supplementary Figure 4).

P210-PAM immunization reduced atherosclerosis in *ApoE*$^{-/-}$ mice

To test the effect of P210-PAM immunization on atherosclerosis, *ApoE*$^{-/-}$ mice were subjected to the same immunization schedule described above and then fed high cholesterol diet from 13 weeks of age until euthanasia at 25 weeks of age. En face Oil-red-O staining of the aorta (Figure 5K) showed significantly reduced aortic atherosclerosis in P210-PAM immunized mice compared to PBS and MSA-PAM immunized mice (Figure 5L). The mean circulating levels of total cholesterol or LDL-C in P210-PAM immunized mice were lower than those in MSA-PAM immunized mice but similar to the mean levels in PBS mice; whereas there was no difference in circulating level of HDL-C among three groups (Supplementary Figure 5A – 5C). There was no difference in IgM or IgG level against P210 among groups but P210-PAM immunized group had reduced IgG1 and IgG2b against P210 (Supplementary Figure 5D - 5G). No differences were observed in the aortic sinus plaque size, lipid stain, and macrophage content (Supplementary Figure 6A - 6I).

P210-PAM immunization reduces IL-1R1 expression and modulates macrophage phenotype

Since P210-PAM immunization elicited an antigen-specific regulation of CD4+ and CD8+ T cells, we next tested if such regulation involved the IL-1β signaling pathway given the known involvement of this pathway in atherosclerosis. There was a significant reduction in splenic IL-1R1, IL-6 and IL-17a gene expression in P210-PAM immunized mice but no difference in IL-1β gene expression when compared to MSA-PAM immunized mice (Figure 5M-5P). Interestingly, the reduced IL-1R1 gene expression was primarily due to decreased expression on splenic F4/80+ cells, but not on CD4+, CD8+ T cells or DCs (Figure 6A-6D), suggesting modulation of macrophages by P210-PAM immunization. To delineate this pathway further, we examined the phenotypes of thioglycolate-induced peritoneal macrophages from P210-PAM or MSA-PAM

immunized mice. The mRNA expression of iNOS, IL-6, IL-12 and IL-10 were all significantly reduced, with a trend toward decreased MCP-1, in macrophages from P210-PAM immunized mice (Figure 6E, 6H-6K). Lack of difference in arginase 1 expression between the groups renders higher arginase 1/iNOS expression ratio in macrophages from P210-PAM immunized mice (Figure 6F, 6G).

$ApoB_{KTTKQSFDL}$ pentamer

The results thus far provide evidence that P210-PAM immunization provokes a response that modulates T cell function and macrophage phenotypes and reduces atherosclerosis in *ApoE*$^{-/-}$ mice, supporting the feasibility of the immunogenic nanoparticle approach to reduce atherosclerosis. However, there are limitations of antigen-based immune-modulation because it depends on the propensity of specific peptides to bind and be presented as immune-antigens by Class-I and Class II MHC. Our previous reports on P210 T cell responses in *ApoE*$^{-/-}$ mice identified Class-I MHC/CD8+ T cell signaling as a mechanism for the protective effects of P210 immunization (4;8). An approach to bridge the experimental investigation towards translational application was therefore developed by screening Class-I HLA propensity to bind P210.

The Human Class-I HLA that occurs with the highest frequency in North America is HLA-A*02:01 and P210 epitope binding to HLA-A*02:01 was tested by ProImmune using the REVEAL assay, which used 9-mer sequential peptides of P210 to assess binding to HLA-A*02:01 (Table 2). The first 9-mer scored well, comparable to the positive control (Figure 7A), suggesting that P210 contains at least one epitope that has the propensity to bind and potentially be presented by HLA-A*02:01, hence a pentamer based on this 9-mer sequence ($ApoB_{KTTKQSFDL}$ pentamer) was

generated for testing. $ApoB_{KTTKQSFDL}$ pentamer was able to detect a small but significant population of P210-specific CD8+ T cells in PBMCs from healthy HLA-A*02:01(+) volunteers (Figure 7B-7E). In 5 out of 8 tested samples, culturing these PBMCs with P210 for 5 days resulted in an increase of pentamer specific CD8+ T cells (Figure 7F-7I).

A2Kb transgenic *ApoE*$^{-/-}$ mice express functional chimeric A2Kb protein

The transgene construct used for developing the mouse model is described in the Methods and Supplementary Method. After obtaining *A2Kb Tg ApoE*$^{-/-}$ offspring from breeding, immunization of male mice with an HLA-A*02:01 restricted hepatitis C virus (HCV) peptide A2V7 significantly increased A2V7-pentamer+ CD8+ T cells in the spleen (P<0.05), compared to adjuvant IFA injected male mice (Figure 8A, 8B). The results demonstrate presentation of the HLA-A*02:01 restricted HCV peptide to activate CD8+ T cells supporting the functional expression of the chimeric transgene. Colony expansion was then undertaken to characterize atherosclerosis in the chimeric model.

High cholesterol diet induces atherosclerosis *in A2Kb Tg ApoE*$^{-/-}$ mice

Feeding female *A2Kb Tg ApoE*$^{-/-}$ mice with high cholesterol diet for 8 weeks starting at 9 weeks of age increased aortic atherosclerosis compared to normal chow feeding (Figure 8C, 8D; 17wk HC and 17wk NC, respectively). High cholesterol diet for 16 weeks significantly increased circulating cholesterol levels (1274 ± 297 mg/dL vs 661 ± 119 mg/dL, P < 0.001 by t-test) and aortic atherosclerosis (6.5 ± 3.0% vs 1.5 ± 1.3%, Figure 8C, 8D; 25wk HC and 25wk NC, respectively) in female mice. Body weight was comparable in female mice fed the two different diets (Supplementary Figure 7A). Similarly, in male mice high cholesterol diet feeding for 8 weeks compared to normal chow significantly increased aortic atherosclerosis (Figure 8C, 8E).

High cholesterol diet for 16 weeks increased circulating cholesterol levels (1760 ± 475 mg/dL vs 617 ± 114 mg/dL, $P < 0.001$ by t-test) and aortic atherosclerosis (8.3 ± 3.2% vs 1.5 ± 1.2%, Figure 8C, 8E). Body weight was also comparable in male mice fed the two different diets (Supplementary Figure 7B). Aortic sinus lesion size was also significantly increased in mice fed high cholesterol diet compared to those fed normal chow (Supplementary Figure 7C, 7D). The results show that aortic atherosclerosis burden is increased by high cholesterol diet in both male and female transgenic mice.

T cell profile and P210-specific T cells in *A2Kb Tg ApoE$^{-/-}$* mice

Feeding *A2Kb Tg ApoE$^{-/-}$* mice with high cholesterol diet for 16 weeks significantly increased CD4+ effector memory T cells without change in central memory T cells in both female and male mice compared to normal chow feeding (Figure 8F- 8I). CD8+ effector memory T cells were also significantly increased in both high cholesterol diet-fed female and male mice. However, feeding high cholesterol diet increased CD8+ central memory T cells significantly in male mice only (Figure 8J – 8M).

The results thus far show that the *A2Kb Tg ApoE$^{-/-}$* mouse is a valid experimental model for atherosclerosis. Given that the results suggest responses are comparable between male and female mice, further analysis combined both sexes for the rest of the studies. $ApoB_{KTTKQSFDL}$ pentamer staining showed that P210 specific CD8+ T cells were increased in *A2Kb Tg ApoE$^{-/-}$* mice fed high cholesterol diet for 8 weeks compared to mice fed normal mouse diet (Figure 8N, P=0.06). P210 specific CD8+ T cells were also observed in the aortic plaque of high cholesterol diet fed mice by flow cytometric analysis of digested whole aortic tissue (Figure 8O). These results support the potential involvement of P210-specific CD8+ T cells in atherosclerosis, in

agreement with our previous studies, and use of $ApoB_{KTTKQSFDL}$ pentamer as a tool to assess P210-specific CD8+ T cell response in atherosclerosis.

P210-PAM induced persistent P210-specific CD8+ T cells in *A2Kb* transgenic mice and reduced atherosclerosis

The results thus far show the *A2Kb Tg ApoE*$^{-/-}$ mouse is a valid humanized atherosclerosis model to investigate translational use of P210-PAM as an antigen-specific immune-modulating therapy. *A2Kb Tg ApoE*$^{-/-}$ mice were immunized as described and were fed high cholesterol diet from 13 weeks of age until euthanasia at 25 weeks of age. We first tested if $ApoB_{KTTKQSFDL}$ pentamer would detect P210-specific CD8+ T cells 13 weeks after the last booster injection. $ApoB_{KTTKQSFDL}$ pentamer positive CD8+ T cells were detected in splenocytes of the immunized mice, trending higher compared to control mice injected with PBS (Figure 9A, P=0.08). Furthermore, *A2Kb Tg ApoE*$^{-/-}$ mice immunized with P210-PAM had significantly reduced aortic atherosclerosis compared to mice injected with PBS (Figure 9B, 9C). An additional group of *A2Kb Tg ApoE*$^{-/-}$ mice were then immunized with MSA-PAM to determine if amphiphilic micelles with a different self-peptide would affect atherosclerosis in the humanized mouse model. There was no significant effect of MSA-PAM on atherosclerosis compared to PBS control, and P210-PAM immunized mice had significantly reduced atherosclerosis compared to MSA-PAM (Figure 9D, 9E). There was no difference of circulating levels of total cholesterol or LDL-C between PBS and P210-PAM immunized mice (Supplementary Figure 8A, 8B), whereas circulating levels of total cholesterol and LDL-C in P210-PAM immunized mice were higher than MSA-PAM immunized mice (Supplementary Figure 8C, 8D). No differences were noted in T cell and macrophage infiltration of the aortas of the immunized *A2Kb Tg ApoE*$^{-/-}$ mice

(Supplementary Figure 8E-H). The results support P210-PAM as a viable translational immune-modulation therapy. The persistence of the P210-specific response can be assessed using a pentamer specific for an epitope of P210.

Discussion

In this study, we report the following novel findings: (a) P210 specific T cell responses exist in human subjects with ASCVD; (b) P210 peptide can be taken up by dendritic cells via proteoglycan binding; (c) P210, when used in a nanoparticle platform (P210-PAM), costains with MHC-I and modulates T cells in *ApoE*$^{-/-}$ mice; (d) In hypercholesterolemic *ApoE*$^{-/-}$ mice, immunization with P210-PAM dampens P210-specific CD4+ T cell proliferative response and CD8+ T cell cytolytic response, modulates macrophage phenotypes, and significantly reduces aortic atherosclerosis; (e) We successfully developed and characterized a humanized atherosclerosis mouse model with *HLA-A*02:01/Kb* chimera in *ApoE*$^{-/-}$ background, serving a translational bridge to potential future human testing; (f) Most importantly, immunization with P210-PAM in the chimeric mice reduced atherosclerosis, indicating P210-PAM is a viable strategy for potential human application. Although P210 has been shown by several investigators as an effective immune-modulation strategy to confer protective effect on atherosclerosis, our studies investigated its use in a nanoparticle formulation, and tested it in humanized chimeric mice to demonstrate potential translational human application.

Investigations on the immune response against various ApoB-100 peptides, including P210, have demonstrated their potential use as peptide antigens for immune modulation therapies (6;38). Although P210 humoral immune response has been demonstrated in human ASCVD (9), information on cellular immune responses against P210 in humans is lacking. One

hallmark feature of antigen-experienced T cells is activation upon antigen rechallenge. Given that patients with ACS have underlying atherosclerotic vascular disease, we tested if there is a population of P210-specific T cells that can be activated upon rechallenge of P210. The AIM assay showed induction of CD69+CD134+ activation markers on CD4+ T cells, supporting the existence of P210-experienced T cells in humans with atherosclerosis. Similarly, we found significantly different responses of CD8+ effector and effector memory T cells to P210 recall stimulation in patients with ACS when compared to those from healthy volunteers. Thus, our data support the notion that cellular immune responses to P210 exist in human ASCVD. Although the causal role of such CD8+ effector memory T cell response in ASCVD remains to be elucidated, it should be noted that memory T cells are enriched in atherosclerotic plaques (39), correlated with atherosclerosis in humans and mouse models (40), and associated with plaque progression and rupture (41). These observations highlight the involvement of memory T cells in atherosclerosis. To our knowledge, this is the first study to demonstrate P210-specific cellular immune responses in human ASCVD.

It is not clear how an auto-immune response to a self-antigen like P210 is triggered. However, the lysine-rich nature of the peptide may provide some insight. A common property of cell penetrating peptides (CPPs) is their cationic nature due to enrichment with lysine and/or arginine residues within the sequences (33;42). CPPs interact with negatively charged cell surface heparin sulfate proteoglycans to gain cell entry (32;33). Interestingly, part of the P210 peptide belongs to the proteoglycan binding domain of the ApoB-100 protein (43;44) and has been shown to be a functioning CPP to generate antigen-specific CD8+ T cell response (34). Our

results provided experimental evidence that P210 indeed has properties of a CPP with proteoglycan-binding properties that facilitates its internalization by DCs.

We have previously demonstrated that the intrinsic CD8+ T cell recall response to P210 stimulation in naïve hypercholesterolemic mice (8). However, it is unknown if the immunologic property of P210 changes when formulated as PAM nanoparticles. We first demonstrated that DCs can uptake P210-PAM and P210 (or its fragment) costains with MHC-I using confocal microscopy. Our observation that P210-PAM immunization increased CD4+CD25+FoxP3+ and CD8+CTLA4+ T cells suggested an induction of regulatory CD4+ and CD8+ T cells. This was further confirmed by functional experiments showing antigen specific reduction of CD4+ T cell proliferative response and CD8+ cytotoxic T cell response to P210. More importantly, P210-PAM immunization significantly reduced aortic atherosclerosis in mice when compared to control groups.

A notable observation is that P210-PAM immunization, in addition to modulating T cells, also modulates macrophages. Interaction between T cells and monocytes/macrophages has been previously reported. CD8+ T cells promote bone marrow monocyte production via IFN-γ mediated mechanism in viral infection (45). Depletion of CD8+ T cells reduced atherosclerosis, decreased the number of mature monocytes in the bone marrow and spleen of hypercholesterolemic mice, reduced GM-CSF and IL-6 expression in bone marrow cells but did not affect the recruitment of monocytes to atherosclerotic plaques (46). In obese tissues, activated CD8+ T cells differentiated peripheral blood monocytes into macrophages (47). CD4+CD25+FoxP3+ T cells have been shown to induce alternatively activated monocytes with reduced inflammatory phenotype (48). Taken together, our data support the notion that P210-

PAM elicits an interaction between T cells and macrophages and reduces the immune-inflammatory responses in atherosclerosis at the level of both innate and adaptive immunity.

The physicochemical properties of nanoparticles play a vital role in determining the immune responses of nanoparticle-based vaccines. Nanoparticles 20-200 nm in diameter are usually internalized by antigen presenting cells to elicit T cell response. Cationic nanoparticles with positive charges facilitate lysosomal escape and cross presentation to MHC-I (49). Solid core nanoparticles with antigen on the surface elicit stronger CD8+ T cell response whereas polymersomes with antigen incorporated inside the core bias toward CD4+ T cell responses. This differential immune response based on physicochemical properties is not strictly dichotomous as reported data has shown solid core nanovaccines can also induce CD4+ T cell response (50). Although cylindrical shaped P210-PAM with P210 on its surface would be predicted to skew toward a CD8 T cell response, our data indicate that P210-PAM elicits regulatory responses in both CD4+ and CD8+ T cells. The concept of delivering autoantigens by nanoparticles to modulate autoimmune diseases has been tested before. The severity of autoantigen induced experimental autoimmune encephalomyelitis or type 1 diabetes can be reduced by this approach (51;52). The beneficial effect was thought to be mediated by promoting differentiation of disease-primed autoreactive CD4+ T cells into T_R1-like cells or by expanding memory-like antidiabetogenic CD8+ T cells, respectively (51;52). Given that P210 is potentially an atherogenic autoantigen, the induction of regulatory T cell responses by P210-PAM is consistent with this view. It should be noted that peptide loaded MHC-II or MHC-I complex was a part of nanoparticles used by Clemente-Casares et al. (51) and Tsai et al. (52), whereas the P210-PAM in this study does not contain MHC molecules.

The mean reduction of atherosclerosis by P210-PAM immunization in the current study was 42% and 37% in *ApoE*$^{-/-}$ mice and *A2Kb Tg ApoE*$^{-/-}$ mice, respectively, consistent with the mean reduction of atherosclerosis between 25% and 60% reported by investigators using different formulations (4-7;11;53-55). Although the reported athero-reduction effect from using various P210 formulation has been consistent across different studies, the reported immune responses to P210 differ. Some reported athero-reduction was associated with increased P210-related antibody production (5-7); some reported induction of regulatory T cell responses (5;11;56). Nevertheless, the reported data supports the notion that P210 is capable of eliciting multiple humoral and cellular immune responses, albeit each study used different dose, preparation, and delivery method of P210.

A few studies have addressed the immune mediators for the athero-reduction effect produced by P210 immunization. Rattik et al. showed B cells pulsed with CTB-P210 reduced atherosclerosis after being transferred into naïve recipients (7), but it is not clear if the B cells functioned as antigen-presenting cells or antibody-producing cells induced by peptide-pulsing. Another study showed that a P210 IgG antibody preparation from rabbits was able to reduce murine atherosclerosis in a passive immunization fashion (57). We previously reported P210 immunization was able to mount antibody response and a CD8 biased T cell response (4). Using a cell transfer strategy, we demonstrated that CD8+ T cells, not B cells or CD4+CD25+ T cells, were the mediators responsible for the athero-protective effect of P210 immunization (4).

The involvement of P210-specific CD8+ T cells described above prompted our investigation to transition towards translational studies. The first step to potentially translate our immunization strategy for clinical testing is to establish if this immunization strategy can

elicit immune response in human subjects. To achieve this, it is necessary to develop tools and models to detect antigen specific T cells and for preclinical end-point testing, respectively. An HLA-A*02:01 based P210 related pentamer, named $ApoB_{KTTKQSFDL}$ pentamer, was generated to track P210-specific CD8+ T cells as a marker for cellular immune response. Using this pentamer, we demonstrated the existence of a small but significant number of antigen specific CD8+ T cells that responded to P210 rechallenge in human PBMCs. We also generated an animal model with a prevalent human MHC-I allele, HLA-A*02:01, to produce proof-of-concept data before advancing this strategy to human testing. We chose HLA-A*02:01 as a representative human MHC-I allele due to its high frequency in the population and generated a new animal model with transgenic expression of human HLA-A*02:01 in *ApoE*$^{-/-}$ mouse on a *C57BL/6J* background. These mice mounted antigen specific CD8+ T cell response to the CD8 restricted peptide A2V7 from human hepatitis C virus as assessed by pentamer after immunization, indicating functional HLA-A*02:01 allele. With P210-PAM immunization, these mice elicited higher splenic $ApoB_{KTTKQSFDL}$ pentamer(+) CD8+ T cells when compared to non-immunized mice. P210-PAM immunization significantly reduced aortic atherosclerosis when compared to control groups, supporting the potential use of P210-PAM for human testing. Given the same genetic background between *ApoE*$^{-/-}$ mouse and chimeric mouse, we speculate P210-PAM immunization modulates macrophages, CD4+ and CD8+ T cells in *A2Kb Tg ApoE*$^{-/-}$ mice similarly to *ApoE*$^{-/-}$ mouse. However, this remains to be confirmed.

The concept of using active immunization strategies to reduce atherosclerosis has progressed in the past three decades. The search for suitable antigens has evolved from using the whole LDL molecule as an antigen to subunits of lipoprotein such as ApoB-100 peptides. In

murine atherosclerosis, immune responses to LDL or its related ApoB-100 peptides are present and modulation of such responses by active immunization with LDL or ApoB-100 peptides confers athero-protective effects. If the same analogy applies to humans, given the existence of immune responses to LDL or ApoB-100 peptides in humans, we hypothesize similar athero-protective effect from active immunization in humans. Here we demonstrate physicochemical and immunological properties of P210-PAM and its effects on T cell responses and atherosclerosis, supporting the use of P210-PAM as an immune-modulation strategy targeting atherosclerosis. Such nanoparticle platforms are suitable for human application as nanoparticle-based vaccines are now in clinical use. More importantly, our successful use of P210-PAM in chimeric mice with human MHC-I allele provided proof-of-concept data showing potential efficacy in human immune system and paves the way for future testing in humans.

Methods

Human PBMC

The protocols were approved by the Cedars-Sinai Institutional Review Board (IRB). Peripheral blood mononuclear cells (PBMCs) were isolated from blood collected from 13 patients with ACS within 72 hours of admission to the Cardiac Intensive Care Unit at Cedars-Sinai Medical Center. Patients were consented under the approved IRB protocol Pro48880. Exclusions were inability to give informed consent, age less than 18 years old, active cancer treated with chemotherapy or radiation, patients taking immune-suppressive drugs, and pregnant women. The data collected was limited to age, sex, LDL levels, and use/non-use of cholesterol-lowering medication (Table 1). PBMCs were isolated using Ficoll (GE Healthcare) density gradient centrifugation and cryo-preserved in commercially available cryogenic solution (Immunospot) in liquid nitrogen. Cryo-preserved PBMCs from healthy controls (N=14) were purchased from a commercial source (Immunospot).

Activation induced marker assay (AIM assay) in human PBMC

Cryo-preserved PBMCs were thawed, rinsed in anti-aggregation solution (Immunospot), and seeded in culture plates at a density of $3x10^6$ cells/ml of RPMI 1640 medium (Invitrogen) supplemented with 10% heat-inactivated pooled human serum (Innovative Research, Inc) and 1X antibiotic/antimycotic (Gibco). After resting for 4 hours, cells were preincubated with 0.5mg/ml anti-CD40 antibody for 15 minutes then stimulated with 20µg/ml P210 peptide, 0.5X T cell stimulation cocktail containing PMA and ionomycin (Thermo Fisher), or CMV (pp65) Peptide Pool (StemCell Tech) as a non-relevant antigen control, whereas cells without treatment served as non-stimulated control. Cells were harvested 16 hours after seeding,

stained for viability (LIVE/DEAD Fixable Aqua Dead Stain Kit, Thermo Fisher), and subjected to cell surface staining for flow cytometry using the following antibodies: CD4, CD8, CD25, CD69, OX40 (CD134), CD137 (4-1 BB) and CD154 (CD40L). Isotypes were used as staining control and eFluor506 labelled CD14, CD16 and CD19 antibodies were used as dump staining to exclude B cells, dendritic cells, macrophages, granulocytes, eosinophil cells and neutrophil cells. The results are expressed as fold change (ratio between the signal in the antigen stimulated condition and the signal in the unstimulated condition) for each subject, consistent with the reported AIM assay (28). Antibodies used in AIM assay are listed in Supplementary Table 1.

Peptide stimulation of human PBMC

Cryo-preserved PBMCs were thawed, rinsed and cultured as in AIM assay but without resting. Cells were stimulated with 20µg/ml P210 peptide or 0.5X T cell stimulation cocktail containing PMA and ionomycin (Thermo Fisher) with non-treated cells serving as negative control. Culture medium was added at $^1/_3$ of the starting volume 48 hours later to replenish the nutrients in the medium. Cells were harvested 72 hours after seeding, stained for viability (LIVE/DEAD Fixable Aqua Dead Stain Kit, Thermo Fisher), and subjected to cell surface staining for flow cytometry using the following antibodies: CD3, CD4, CD8, CD45RA, CD45RO, CD62L, and CD197 (CCR7). Isotypes were used as staining control. CD4+ or CD8+ T Effector cells were gated on CD45RO+CD62L(-)CD197(-). T Effector Memory cells were CD45RO+CD45RA(-)CD62L(-)CD197(-). Antibodies used are listed in Supplementary Table 2. Results were tabulated as Response Index using the following calculation:

(% peptide stimulation - % no stimulation)/(% cocktail stimulation) X 100

The results are expressed as Response Index to account for inherent variations introduced by culturing cells in vitro over time, controlled for by assessing response relative to baseline cell phenotype (% no stimulation) and maximal stimulation (% cocktail stimulation) for each subject PBMC (58). Each data point represents one subject.

Animals

All mice were maintained under standard animal housing conditions with a 12-h light-dark cycle and were fed ad libitum with a regular chow diet (5015, PMI Nutrition International, USA) unless mentioned otherwise. All animal procedures were done in compliance with National Institutes of Health guidelines and were approved by IACUC. *B6.129P2-Apoe^{tm1Unc}/J* (*ApoE$^{-/-}$*) mice were purchased from Jackson Lab (Stock No: 002052, Bar Harbor, Me). A2Kb transgenic *CB6F1-Tg(HLA-A*02:01/H2-Kb)A*0201* mice were purchased from Taconic Biosciences (Model 9659).

Amphiphile synthesis, assembly and characterization

See Supplemental Method for details.

Dendritic cell uptake of FITC labelled P210 and P210-PAM

P210 peptide was labelled with FITC using a commercially available kit (Thermo Fisher). To prepare FITC-P210-PAM, P210 peptide was first labeled with FITC on the last lysine on C-terminal when the peptide was synthesized, then the labelled P210-FITC were assembled to FITC-P210-PAM using methods described in the Supplementary Method for micelle assembly.

Bone marrow derived dendritic cells (BMDCs) were prepared using BM cells from femurs and tibiae of male *ApoE$^{-/-}$* mice. After depletion of erythrocytes with lysis buffer, BM cells were cultured in 10cm dishes with 10ml complete RPMI-1640 medium supplemented with

20ng/ml GM-CSF (R&D Systems) and 10 ng/ml IL-4 (Invitrogen). On Day 2, 10ml fresh culture medium was added to each dish, then 10ml medium was replaced with fresh medium on day 4 and 6. On day 8, non-adherent immature denritic cells were harvested into new culture medium containing 100µg/ml P210-FITC or FITC-P210-PAM in complete RPMI-1640 medium. After a 4h incubation for P210-FITC or 6h incubation for FITC-P210-PAM, cells were collected and stained with antibodies to CD11c (N418, Invitrogen)or CD11c and H2-K^b (AF6-88.5.5.3, Invitrogen), respectively. Cells were washed and fixed in 4% paraformaldehyde followed by washing and staining with the fluorescent nuclear stain Hoechst 33342 (Thermofisher) or DAPI (Invitrogen). Washed cells were then smeared on a slide, briefly air-dried in the dark, and fixed in cold acetone. Photographs were then taken on a Leica or Zeiss confocal microscope visualized with liquid fluorescent mounting medium. Untreated DC were collected and smeared on slides, air dried, then stained with Giemsa staining reagent (Beckman Coulter) according to the kit instruction with photos taken using light microscope to demonstrate dendrites.

For flow cytometric experiments, P210-FITC uptake was assessed after a 2h incubation and staining for CD11c. For heparin binding experiments, 100µg/mL P210-FITC was pre-incubated with 100 U/mL heparin for 30 minutes at room temperature and centrifuged at 1000 x *g* for 5 min. The supernatant was carefully removed and added to the cell culture. Cells were collected after 2h and stained for CD11c for flow cytometry. In a separate experiment, DCs were treated with p-nitrophenyl-β-D-xylopyranoside (pNP-xyl), a competitive inhibitor of heparan sulfate chain addition, for 18 hours at a final concentration of 3 mM. DCs were then

incubated with P210-FITC for 2 hours, collected, and stained with anti-CD11c (N418) for flow cytometry.

PAM biodistribution in vivo

The *in vivo* biodistribution of P210-PAM or MSA-PAM was evaluated by injecting 1 mM cy7-labeled PAMs in 100 µl volume subcutaneously into the scruff of the neck in *C57BL/6J* mice (n = 4). After injection, mice were shaved and imaged over 7 days (168 h) using an AMI HTX imaging system (Spectral Instruments Tucson, AZ, USA). A separate group of mice was euthanized 48 hrs after injection to harvest injection site for immunostaining.

T cell immune response to P210-PAM in naïve hypercholesterolemic mice

Splenocytes were collected from 25 week old *ApoE*$^{-/-}$ mice euthanized after 16 weeks of high cholesterol diet feeding consisting of 0.15% cholesterol, 21% fat (TD.88137, Envigo). RBC lysed splenocytes were incubated with 20 µg/ml P210-PAM in complete RPMI-1640 medium for 48h then stained with CD3e (145-2C11, eBioscience), CD4 (GK1.5, BD Bioscience), CD8b (H35-17.2, eBioscience), CD44 (IM7, eBioscience) and CD62L (MEL-I4, eBioscience) antibodies for T effector/memory cell profiling using flow cytometry.

Immunization with P210-PAM and phenotyping atherosclerotic lesions

Seven week old *ApoE*$^{-/-}$ mice fed normal chow received a subcutaneous injection of one of the following: P210-PAM, MSA-PAM, or PBS. PAM dose used was 100 µg/mouse. Booster injections were administered at 10 and 12 weeks of age. Some mice were euthanized one week after the second booster for immune profiling. The rest of the mice were fed high cholesterol diet for 12 weeks and euthanized at 25 weeks of age. Whole aortas were cleaned, processed and stained with Oil-red-O to assess the extent of atherosclerosis *en face*. Frozen heart bases

embedded in OCT (Optimum Cutting Temperature, Tissue-Tek) were cryo-sectioned starting from the appearance of 3 complete aortic valves. Three slides with 2 sections on each slide at 4-5 slides intervals were grouped for aortic sinus histomorphometry. Plaque sizes and lipid content were accessed by Oil-Red-O staining using standard protocol. Macrophage in atherosclerotic lesions in the aortic sinus was assessed by immunohistochemistry staining with anti-CD68 (FA-11, BioLegend) antibody, following with incubation with appropriate secondary antibody using standard protocol. Computer-assisted morphometric analysis was performed by a blinded observer using ImagePro (ImagePro Plus, version 4.0, Media Cybernetics Inc., Rockville, Maryland). Serum levels of total cholesterol, LDL-C and HDL-C were measured using commercially availabe kits according to manufacturer's instruction (Wako).

ELISA for P210 antibodies

Flat-bottomed 96-well polystyrene plates (MaxiSorp, Germany) were pre-coated with 100 ul P210 (20 μg/ml) in Na_2CO_3-$NaHCO_3$ buffer (pH9.6) overnight at 4°C to assess antibody levels using standard protocol. The coating concentration and serum dilution was optimized in pilot experiments. Goat anti-mouse HRP -IgG (Pierce), IgM (Southern Biotech), rat anti mouse-IgG1-HRP (Invitrogen) and goat anti mouse-IgG2b -HRP (Southern Biotech) were used as detecting antibodies and the bound antibodies were detected by developing in ABTS (Southern Biotech) as substrate and optical density values were recorded at 405 nm. Given there is no purified P210 antibody that can be used for standardization, OD of individual mouse in each group was normalized against the mean OD from PBS group and presented as "adjusted O.D." in the figures.

Immune profile of P210-PAM immunized mice

Splenocytes of immunized *ApoE*$^{-/-}$ mice that were euthanized at 13 weeks of age (1 week after second booster) were subjected to RBC lysis. An aliquot of splenocytes were stained for CD4 (GK1.5, BD Bioscience), CD8 (YTS156.7.7, BioLegend), CD25 (PC61.5, eBioscience), CTLA-4 (UC10-4B9, BioLegend), FoxP3 (R16-715, BD Bioscience), and PD-1 (29F 1A12, BioLegend) and analyzed by flow cytometry excluding non-viable cells. A second aliquot was used to assess cytolytic activity using CD107a (1D4B) staining. Briefly, splenocytes were incubated in complete RPMI-1640 medium with 2.5 μg/ml fluorescent CD107a antibody and 5 μg/ml P210 for 1h. Monensin (1x) was added and the cells incubated for another 4 hours. Cells were then collected and stained with fluorescent CD3e (145-2C11, BD Pharmingen) and CD8b (H35-17.2, Invitrogen) antibodies. The cells were analyzed by flow cytometer excluding non-viable cells. T cell proliferation was assessed using BrdU. Briefly, splenocytes were cultured in complete RPMI-1640 medium at $2.5x10^6$ cells/ml and stimulated with P210 (20 μg/ml). Cells stimulated with Concanavalin A (2.5 μg/ml) served as positive control. Untreated cells served as baseline controls. After 48h, BrdU was added at a final concentration of 10 μM. Cells were collected after 24h and stained for CD3e (BM10-37, BD Bioscience), CD4 (GK1.5, BD Bioscience), CD8b (H35-17.2, Invitrogen) and BrdU (3D4, BD Pharmingen) according to manufacturer's instructions (BrdU Flow Kit, BD Pharmingen) then analyzed by flow cytometry. Proliferation index was calculated as [(%BRDU+ cells in P210 peptide stimulation - %BRDU+ cells in no stimulation)/(%BRDU+ cells in Con A stimulation)] X 100.

Induction of peritoneal macrophages

Seven weeks old *ApoE*$^{-/-}$ mice fed normal chow were immunized as previously described. At 13 weeks of age (1 week after second booster), mice received peritoneal injection of 1ml 3%

thioglycollate medium (in PBS) and cells from peritoneal cavity were harvested 72hrs after injection. Cells were seeded to culture dish and incubated at 37^0C for 4hrs to obtain attached peritoneal macrophages.

qPCR

Total RNA was extracted from spleens or peritoneal macrophages enriched from peritoneal exudate by pre-attaching to culture plates using TRIzol (Thermo Fisher). cDNA synthesis and quantitative real-time PCR were then performed using SuperScript VILO cDNA Synthesis Kit (Thermo Fisher), and iTaq Universal SYBR Green Supermix and iQ5 Real-Time PCR Detection System (Bio-Rad), respectively, per manufacturers' protocols. GAPDH served as the reference gene and results were expressed as fold-change relative to non-treated cells of each sample using the $Ct_{\Delta\Delta}$ method. Primer sequences used for qPCR are listed in Supplementary Table 3.

Detection of $ApoB_{KTTKQSFDL}$ Pentamer (+) CD8+ T cells in human PBMCs

Proimmune was contracted to screen for potential binding epitopes in P210 to HLA-A*02:01. First 9-mer sequence in P210 was found to have high binding score and an HLA-A*02:01 pentamer based on this 9-mer sequence, named $ApoB_{KTTKQSFDL}$ pentamer, was then purchased from Proimmune. For pentamer staining, commercially available HLA-A*02:01 typed cryo-preserved PBMCs (Immunospot) were thawed, rinsed in anti-aggregation solution (Immunospot) and divided into $2x10^6$ cell aliquots. $ApoB_{KTTKQSFDL}$ pentamer staining was performed according to manufacturer's instruction, with the HLA-A*02:01 Negative Pentamer (ProImmune) as negative control. Each sample stained for $ApoB_{KTTKQSFDL}$ pentamer had its corresponding negative control stain. Cells were washed and then stained for CD8 (LT8) and

CD19 (HIB19). Cells were again washed after staining and resuspended in 1% paraformaldehyde in 1% BSA/0.1% sodium azide and analyzed. $ApoB_{KTTKQSFDL}$ pentamer positive cells for each sample were determined based on the corresponding Negative Pentamer.

_A2Kb_ transgenic _ApoE_$^{-/-}$ mice

A2Kb Tg ApoE$^{-/-}$ mice were generated as briefly described below (See Supplementary Method for details). A 3867 bp full-length chimeric *A2Kb* gene was cloned into pCR-XL-TOPO T vector (Thermo Fisher) and the amplified recombinant plasmids containing *A2Kb* gene were digested with restriction enzymes to yield ~3.9-kb fragments containing the chimeric *A2Kb* gene for fertilized *ApoE*$^{-/-}$ eggs microinjection by the Cedars Sinai Rodent Genetics Core. Germline-transmitted A2Kb chimeras obtained were screened by PCRs detecting *HLA-A*02:01* fragments and flow cytometric analysis of *A2Kb* protein expression on the surface of peripheral blood mononuclear cells (PBMCs).

A transgenic *ApoE*$^{-/-}$ male mouse was identified and crossbred with female *ApoE*$^{-/-}$ mice. The *A2Kb* transgenic offspring selected by flow cytometric analysis of chimeric A2Kb protein expression on peripheral blood cells were used for further breeding or experiments.

Functional expression of _A2Kb_ transgene

Male *A2Kb Tg ApoE*$^{-/-}$ mice were immunized with the *HLA-A*02:01* restricted peptide A2V7 from human hepatitis C virus (HCV NS5a 1987–1995, VLSDFKTWL; ProImmune) emulsified in incomplete Freund's adjuvant (IFA; MP Biomedicals) at 9 and 10 weeks of age by subcutaneous injection at a dose of 20ug/100ul. Mice immunized with 100ul IFA alone served as control. Mice were euthanized at 11 weeks of age. HLA-A*02:01 restricted antigen specific immune response was evaluated by flow cytometric analysis of splenocytes stained with CD19

(6D5, BioLegend), CD8α (KT15, GeneTex), and PE-conjugated HLA-A*02:01/A2V7- pentamer (ProImmune).

Atherosclerosis in *A2Kb Tg ApoE$^{-/-}$* mice

A2Kb Tg ApoE$^{-/-}$ mice were divided into two groups and fed normal chow or high cholesterol diet starting at 9 weeks of age until euthanasia at 17 or 25 weeks of age. RBC lysed splenocytes were stained for T effector/memory cell profile.

Another cohort of high cholesterol diet fed mice were euthanized at 17 weeks of age and the splenocytes stained with CD19 (6D5), CD8α (KT15), and PE-conjugated $ApoB_{KTTKQSFDL}$ pentamer (ProImmune). A third cohort of female *A2Kb Tg ApoE$^{-/-}$* mice aged 66-68 weeks were fed high cholesterol diet for 4 weeks and euthanized to collect the whole aorta for enzymatic digestion with 0.25 mg/ml Collagenase, 0.125 mg/ml Elastase, and 60 U/ml Hyaluronidase (Sigma-Aldrich) in sterile RPMI 1640 medium for 20 minutes at 37°C. Single cell suspensions were then stained for $ApoB_{KTTKQSFDL}$ pentamer and flow cytometric analysis as described above.

Immunization with P210-PAM in *A2Kb* transgenic mice

The first cohort of *A2Kb Tg ApoE$^{-/-}$* mice received either PBS or P210-PAM according to the same immunization protocol described prior for *ApoE$^{-/-}$* mice. Mice were sacrificed at 25 weeks of age and splenocytes were subject to flow cytometric analysis of $ApoB_{KTTKQSFDL}$ pentamer (+) CD8+ T cells and their aorta for morphometric analysis of Oil-red-O (+) plaques. To have a proper control for P210-PAM immunization, a second cohort of *A2Kb Tg ApoE$^{-/-}$* mice were immunized with MSA-PAM or P210-PAM using the same protocol and aorta analyzed for Oil-red-O (+) plaques.

Statistics

Data are presented as mean ± SD. Number of animals in each group and statistical methods are listed in text, figures or figure legend. $P \leq 0.05$ was considered as statistically significant but trending data were also noted.

Study approval

The protocols for human studies were approved by the Cedars-Sinai Institutional Review Board (IRB) with patients consented under the approved IRB protocol Pro48880. Exclusions were inability to give informed consent, age less than 18 years old, active cancer treated with chemotherapy or radiation, patients taking immune-suppressive drugs, and pregnant women. Animal protocols were approved by IACUC at Cedars-Sinai Medical Center and all animal procedures were done in compliance with National Institutes of Health guidelines.

Author contributions

KYC, XZ, JZ, PCD, NT and EJC contributed to the designing experiments, analyzing and interpreting data, writing and revising the manuscript.

XZ, JZ, NWML and NT contributed to conducting experiments, acquiring data.

NT and EJC provided nanoparticle vaccines for the studies.

BC contributed to the establishing IRB protocol and acquisition of human PBMCs, writing and revising the manuscript.

PKS contributed to the conceptualization of the study, interpretation of the data, writing and revising the manuscript.

Acknowledgement

This study was supported by TheHeartFoundation, Eisner Foundation, Peterson foundation, Corday Foundation and Spielberg fund. The authors would also like to acknowledge the financial support from the National Heart, Lung, and Blood Institute (NHLBI, R00HL124279), NIH Director's New Innovator Award (DP2-DK121328), and the University of Southern California Women in Science and Engineering (WiSE) Major Support Award awarded to EJC. The authors also thank Juliana Yano and Mingtian Che for their excellent technical support in this project.

Reference List

1. Ketelhuth,D.F., and Hansson,G.K. 2016. Adaptive Response of T and B Cells in Atherosclerosis. *Circ. Res.* **118**:668-678.

2. Chistiakov,D.A., Orekhov,A.N., and Bobryshev,Y.V. 2016. Immune-inflammatory responses in atherosclerosis: Role of an adaptive immunity mainly driven by T and B cells. *Immunobiology* **221**:1014-1033.

3. Ma,S.D., Mussbacher,M., and Galkina,E.V. 2021. Functional Role of B Cells in Atherosclerosis. *Cells* **10**:doi: 10.3390/cells10020270.

4. Chyu,K.Y., Zhao,X., Dimayuga,P.C., Zhou,J., Li,X., Yano,J., Lio,W.M., Chan,L.F., Kirzner,J., Trinidad,P. et al 2012. CD8+ T cells mediate the athero-protective effect of immunization with an ApoB-100 peptide. *PLoS. ONE.* **7**:e30780.

5. Klingenberg,R., Lebens,M., Hermansson,A., Fredrikson,G.N., Strodthoff,D., Rudling,M., Ketelhuth,D.F., Gerdes,N., Holmgren,J., Nilsson,J. et al 2010. Intranasal Immunization With an Apolipoprotein B-100 Fusion Protein Induces Antigen-Specific Regulatory T Cells and Reduces Atherosclerosis. *Arterioscler. Thromb. Vasc. Biol.* **30**:946-952.

6. Fredrikson,G.N., Soderberg,I., Lindholm,M., Dimayuga,P., Chyu,K.Y., Shah,P.K., and Nilsson,J. 2003. Inhibition of atherosclerosis in apoE-null mice by immunization with apoB-100 peptide sequences. *Arterioscler. Thromb. Vasc. Biol.* **23**:879-884.

7. Rattik,S., Mantani,P.T., Yao,M., I, Ljungcrantz,I., Sundius,L., Bjorkbacka,H., Terrinoni,M., Lebens,M., Holmgren,J., Nilsson,J. et al 2018. B cells treated with CTB-p210 acquire a regulatory phenotype in vitro and reduce atherosclerosis in apolipoprotein E deficient mice. *Vascul. Pharmacol.* **111**:54-61.

8. Dimayuga,P.C., Zhao,X., Yano,J., Lio,W.M., Zhou,J., Mihailovic,P.M., Cercek,B., Shah,P.K., and Chyu,K.Y. 2017. Identification of apoB-100 Peptide-Specific CD8+ T Cells in Atherosclerosis. *J. Am. Heart Assoc.* **6**:doi: 10.1161/JAHA.116.005318.

9. Sjogren,P., Fredrikson,G.N., Samnegard,A., Ericsson,C.G., Ohrvik,J., Fisher,R.M., Nilsson,J., and Hamsten,A. 2008. High plasma concentrations of autoantibodies against native peptide 210 of apoB-100 are related to less coronary atherosclerosis and lower risk of myocardial infarction. *Eur. Heart J.* **29**:2218-2226.

10. Mayr,M., Grainger,D., Mayr,U., Leroyer,A.S., Leseche,G., Sidibe,A., Herbin,O., Yin,X., Gomes,A., Madhu,B. et al 2009. Proteomics, metabolomics, and immunomics on microparticles derived from human atherosclerotic plaques. *Circ. Cardiovasc. Genet.* **2**:379-388.

11. Herbin,O., it-Oufella,H., Yu,W., Fredrikson,G.N., Aubier,B., Perez,N., Barateau,V., Nilsson,J., Tedgui,A., and Mallat,Z. 2012. Regulatory T-cell response to apolipoprotein

B100-derived peptides reduces the development and progression of atherosclerosis in mice. *Arterioscler. Thromb. Vasc. Biol.* **32**:605-612.

12. Gupta,R.K. 1998. Aluminum compounds as vaccine adjuvants. *Adv. Drug Deliv. Rev.* **32**:155-172.

13. Wang,Z.B., and Xu,J. 2020. Better Adjuvants for Better Vaccines: Progress in Adjuvant Delivery Systems, Modifications, and Adjuvant-Antigen Codelivery. *Vaccines. (Basel)* **8**:128.

14. Pierides,C., Bermudez-Fajardo,A., Fredrikson,G.N., Nilsson,J., and Oviedo-Orta,E. 2013. Immune responses elicited by apoB-100-derived peptides in mice. *Immunol. Res.* **56**:96-108.

15. Anselmo,A.C., and Mitragotri,S. 2021. Nanoparticles in the clinic: An update post COVID-19 vaccines. *Bioeng. Transl. Med.* **6**:e10246.

16. Lung,P., Yang,J., and Li,Q. 2020. Nanoparticle formulated vaccines: opportunities and challenges. *Nanoscale.* **12**:5746-5763.

17. Cervadoro,A., Palomba,R., Vergaro,G., Cecchi,R., Menichetti,L., Decuzzi,P., Emdin,M., and Luin,S. 2018. Targeting Inflammation With Nanosized Drug Delivery Platforms in Cardiovascular Diseases: Immune Cell Modulation in Atherosclerosis. *Front Bioeng. Biotechnol.* **6**:177.

18. Flores,A.M., Ye,J., Jarr,K.U., Hosseini-Nassab,N., Smith,B.R., and Leeper,N.J. 2019. Nanoparticle Therapy for Vascular Diseases. *Arterioscler. Thromb. Vasc. Biol.* **39**:635-646.

19. Bejarano,J., Navarro-Marquez,M., Morales-Zavala,F., Morales,J.O., Garcia-Carvajal,I., raya-Fuentes,E., Flores,Y., Verdejo,H.E., Castro,P.F., Lavandero,S. et al 2018. Nanoparticles for diagnosis and therapy of atherosclerosis and myocardial infarction: evolution toward prospective theranostic approaches. *Theranostics.* **8**:4710-4732.

20. Chin,D.D., Poon,C., Wang,J., Joo,J., Ong,V., Jiang,Z., Cheng,K., Plotkin,A., Magee,G.A., and Chung,E.J. 2021. miR-145 micelles mitigate atherosclerosis by modulating vascular smooth muscle cell phenotype. *Biomaterials* **273**:120810.

21. Chin,D.D., Poon,C., Trac,N., Wang,J., Cook,J., Joo,J., Jiang,Z., Sta Maria,N.S., Jacobs,R.E., and Chung,E.J. 2020. Collagenase-Cleavable Peptide Amphiphile Micelles as a Novel Theranostic Strategy in Atherosclerosis. *Adv. Therap* **3**:1900196.

22. Kelly,C.P., Murray,J.A., Leffler,D.A., Getts,D.R., Bledsoe,A.C., Smithson,G., First,M.R., Morris,A., Boyne,M., Elhofy,A. et al 2021. TAK-101 Nanoparticles Induce Gluten-Specific Tolerance in Celiac Disease: A Randomized, Double-Blind, Placebo-Controlled Study. *Gastroenterology* **161**:66-80.

23. Joo,J., Poon,C., Yoo,S.P., and Chung,E.J. 2018. Shape Effects of Peptide Amphiphile Micelles for Targeting Monocytes. *Molecules.* **23**:2786.

24. Trac,N.T., and Chung,E.J. 2020. Peptide-based targeting of immunosuppressive cells in cancer. *Bioact. Mater.* **5**:92-101.

25. Trac,N., Chen,L.Y., Zhang,A., Liao,C.P., Poon,C., Wang,J., Ando,Y., Joo,J., Garri,C., Shen,K. et al 2021. CCR2-targeted micelles for anti-cancer peptide delivery and immune stimulation. *J. Control Release* **329**:614-623.

26. Dan,J.M., Lindestam Arlehamn,C.S., Weiskopf,D., da Silva,A.R., Havenar-Daughton,C., Reiss,S.M., Brigger,M., Bothwell,M., Sette,A., and Crotty,S. 2016. A Cytokine-Independent Approach To Identify Antigen-Specific Human Germinal Center T Follicular Helper Cells and Rare Antigen-Specific CD4+ T Cells in Blood. *J. Immunol.* **197**:983-993.

27. Jiang,W., Wragg,K.M., Tan,H.X., Kelly,H.G., Wheatley,A.K., Kent,S.J., and Juno,J.A. 2019. Identification of murine antigen-specific T follicular helper cells using an activation-induced marker assay. *J. Immunol. Methods* **467**:48-57.

28. Reiss,S., Baxter,A.E., Cirelli,K.M., Dan,J.M., Morou,A., Daigneault,A., Brassard,N., Silvestri,G., Routy,J.P., Havenar-Daughton,C. et al 2017. Comparative analysis of activation induced marker (AIM) assays for sensitive identification of antigen-specific CD4 T cells. *PLoS. ONE.* **12**:e0186998.

29. Fredrikson,G.N., Anand,D.V., Hopkins,D., Corder,R., Alm,R., Bengtsson,E., Shah,P.K., Lahiri,A., and Nilsson,J. 2009. Associations between autoantibodies against apolipoprotein B-100 peptides and vascular complications in patients with type 2 diabetes. *Diabetologia.* **52**:1426-1433.

30. McLeod,O., Silveira,A., Fredrikson,G.N., Gertow,K., Baldassarre,D., Veglia,F., Sennblad,B., Strawbridge,R.J., Larsson,M., Leander,K. et al 2014. Plasma autoantibodies against apolipoprotein B-100 peptide 210 in subclinical atherosclerosis. *Atherosclerosis* **232**:242-248.

31. Hansson,G.K., and Hermansson,A. 2011. The immune system in atherosclerosis. *Nat. Immunol.* **12**:204-212.

32. Poon,G.M., and Gariepy,J. 2007. Cell-surface proteoglycans as molecular portals for cationic peptide and polymer entry into cells. *Biochem. Soc. Trans.* **35**:788-793.

33. Brooks,N.A., Pouniotis,D.S., Tang,C.K., Apostolopoulos,V., and Pietersz,G.A. 2010. Cell-penetrating peptides: application in vaccine delivery. *Biochim. Biophys. Acta* **1805**:25-34.

34. Sakamoto,N., and Rosenberg,A.S. 2011. Apolipoprotein B binding domains: evidence that they are cell-penetrating peptides that efficiently deliver antigenic peptide for cross-presentation of cytotoxic T cells. *J. Immunol.* **186**:5004-5011.

35. Wilsie,L.C., Chanchani,S., Navaratna,D., and Orlando,R.A. 2005. Cell surface heparan sulfate proteoglycans contribute to intracellular lipid accumulation in adipocytes. *Lipids Health Dis.* **4**:2.

36. Ikenaga,T., Yamasaki,Y., Shakushiro,K., Nishikawa,M., and Takakura,Y. 2004. Induction of cytotoxic T lymphocytes following immunization with cationized soluble antigen. *Vaccine* **22**:2609-2616.

37. Moyer,T.J., Zmolek,A.C., and Irvine,D.J. 2016. Beyond antigens and adjuvants: formulating future vaccines. *J. Clin. Invest* **126**:799-808.

38. Chyu,K.Y., Zhao,X., Reyes,O.S., Babbidge,S.M., Dimayuga,P.C., Yano,J., Cercek,B., Fredrikson,G.N., Nilsson,J., and Shah,P.K. 2005. Immunization using an Apo B-100 related epitope reduces atherosclerosis and plaque inflammation in hypercholesterolemic apo E (-/-) mice. *Biochem. Biophys. Res. Commun.* **338**:1982-1989.

39. Fernandez,D.M., Rahman,A.H., Fernandez,N.F., Chudnovskiy,A., Amir,E.D., Amadori,L., Khan,N.S., Wong,C.K., Shamailova,R., Hill,C.A. et al 2019. Single-cell immune landscape of human atherosclerotic plaques. *Nat. Med.* **25**:1576-1588.

40. Ammirati,E., Cianflone,D., Vecchio,V., Banfi,M., Vermi,A.C., De,M.M., Grigore,L., Pellegatta,F., Pirillo,A., Garlaschelli,K. et al 2012. Effector Memory T cells Are Associated With Atherosclerosis in Humans and Animal Models. *J. Am. Heart Assoc.* **1**:27-41.

41. van Dijk,R.A., Duinisveld,A.J., Schaapherder,A.F., Mulder-Stapel,A., Hamming,J.F., Kuiper,J., de Boer,O.J., van der Wal,A.C., Kolodgie,F.D., Virmani,R. et al 2015. A change in inflammatory footprint precedes plaque instability: a systematic evaluation of cellular aspects of the adaptive immune response in human atherosclerosis. *J. Am. Heart Assoc.* **4**:e001403.

42. Chua,B.Y., Eriksson,E.M., Poole,D.P., Zeng,W., and Jackson,D.C. 2008. Dendritic cell acquisition of epitope cargo mediated by simple cationic peptide structures. *Peptides* **29**:881-890.

43. Olsson,U., Camejo,G., Hurt-Camejo,E., Elfsber,K., Wiklund,O., and Bondjers,G. 1997. Possible functional interactions of apolipoprotein B-100 segments that associate with cell proteoglycans and the ApoB/E receptor. *Arterioscler. Thromb. Vasc. Biol.* **17**:149-155.

44. Segrest,J.P., Jones,M.K., De,L.H., and Dashti,N. 2001. Structure of apolipoprotein B-100 in low density lipoproteins. *J. Lipid Res.* **42**:1346-1367.

45. Schúrch,C.M., Riether,C., and Ochsenbein,A.F. 2014. Cytotoxic CD8+ T cells stimulate hematopoietic progenitors by promoting cytokine release from bone marrow mesenchymal stromal cells. *Cell Stem Cell* **14**:460-472.

46. Cochain,C., Koch,M., Chaudhari,S.M., Busch,M., Pelisek,J., Boon,L., and Zernecke,A. 2015. CD8+ T Cells Regulate Monopoiesis and Circulating Ly6C-high Monocyte Levels in Atherosclerosis in Mice. *Circ. Res.* **117**:244-253.

47. Nishimura,S., Manabe,I., Nagasaki,M., Eto,K., Yamashita,H., Ohsugi,M., Otsu,M., Hara,K., Ueki,K., Sugiura,S. et al 2009. CD8+ effector T cells contribute to macrophage recruitment and adipose tissue inflammation in obesity. *Nat. Med.* **15**:914-920.

48. Romano,M., Fanelli,G., Tan,N., Nova-Lamperti,E., McGregor,R., Lechler,R.I., Lombardi,G., and ScottÃ ,C. 2018. Expanded Regulatory T Cells Induce Alternatively Activated Monocytes With a Reduced Capacity to Expand T Helper-17 Cells. *Front Immunol.* **9**:1625.

49. Kim,C.G., Kye,Y.C., and Yun,C.H. 2019. The Role of Nanovaccine in Cross-Presentation of Antigen-Presenting Cells for the Activation of CD8(+) T Cell Responses. *Pharmaceutics.* **11**:612.

50. Stano,A., Scott,E.A., Dane,K.Y., Swartz,M.A., and Hubbell,J.A. 2013. Tunable T cell immunity towards a protein antigen using polymersomes vs. solid-core nanoparticles. *Biomaterials* **34**:4339-4346.

51. Clemente-Casares,X., Blanco,J., Ambalavanan,P., Yamanouchi,J., Singha,S., Fandos,C., Tsai,S., Wang,J., Garabatos,N., Izquierdo,C. et al 2016. Expanding antigen-specific regulatory networks to treat autoimmunity. *Nature* **530**:434-440.

52. Tsai,S., Shameli,A., Yamanouchi,J., Clemente-Casares,X., Wang,J., Serra,P., Yang,Y., Medarova,Z., Moore,A., and Santamaria,P. 2010. Reversal of autoimmunity by boosting memory-like autoregulatory T cells. *Immunity.* **32**:568-580.

53. Fredrikson,G.N., Bjorkbacka,H., Soderberg,I., Ljungcrantz,I., and Nilsson,J. 2008. Treatment with apo B peptide vaccines inhibits atherosclerosis in human apo B-100 transgenic mice without inducing an increase in peptide-specific antibodies. *J. Intern. Med.* **264**:563-570.

54. Yi,S., Zhang,X., Sangji,H., Liu,Y., Allen,S.D., Xiao,B., Bobbala,S., Braverman,C.L., Cai,L., Hecker,P.I. et al 2019. Surface engineered polymersomes for enhanced modulation of dendritic cells during cardiovascular immunotherapy. *Adv. Funct. Mater* **29**.

55. Yi,X., Wang,Y., Jia,Z., Hiller,S., Nakamura,J., Luft,J.C., Tian,S., and DeSimone,J.M. 2020. Retinoic Acid-Loaded Poly(lactic-co-glycolic acid) Nanoparticle Formulation of ApoB-100-Derived Peptide 210 Attenuates Atherosclerosis. *J. Biomed. Nanotechnol.* **16**:467-480.

56. Wigren,M., Kolbus,D., Duner,P., Ljungcrantz,I., Soderberg,I., Bjorkbacka,H., Fredrikson,G.N., and Nilsson,J. 2010. Evidence for a role of regulatory T cells in mediating the atheroprotective effect of apolipoprotein B peptide vaccine. *J. Intern. Med.* **269**:546-556.

57. Zeng,Z., Cao,B., Guo,X., Li,W., Li,S., Chen,J., Zhou,W., Zheng,C., and Wei,Y. 2018. Apolipoprotein B-100 peptide 210 antibody inhibits atherosclerosis by regulation of macrophages that phagocytize oxidized lipid. *Am. J. Transl. Res.* **10**:1817-1828.

58. Chernomordik,F., Cercek,B., Lio,W.M., Mihailovic,P.M., Yano,J., Herscovici,R., Zhao,X., Zhou,J., Chyu,K.Y., Shah,P.K. et al 2020. The Role of T Cells Reactive to the Cathelicidin Antimicrobial Peptide LL-37 in Acute Coronary Syndrome and Plaque Calcification. *Front Immunol.* **11**:575577.

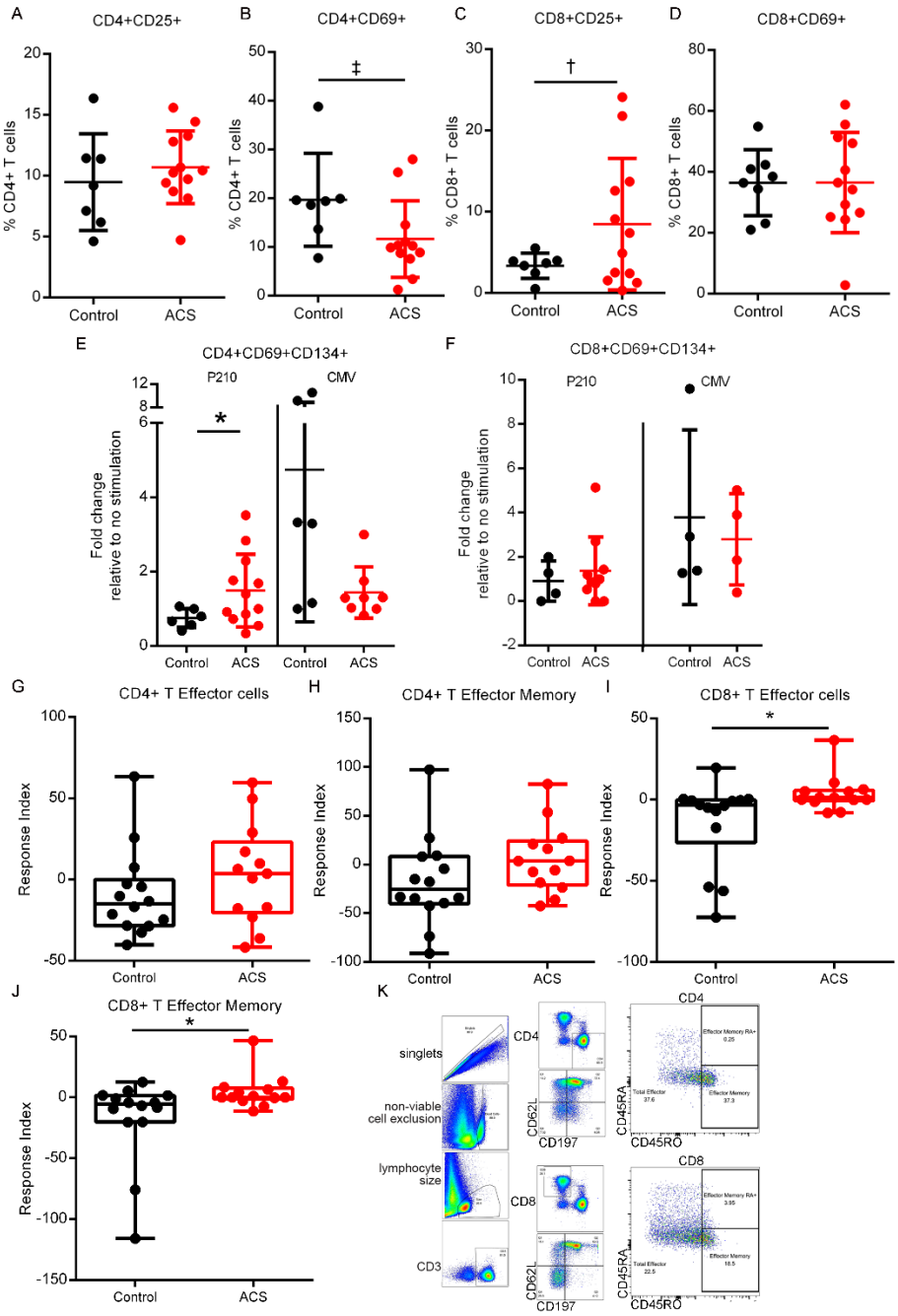

Figure 1: Intrinsic T cell response to P210 peptide in human PBMCs. Human peripheral blood mononuclear cells from control subjects and acute coronary syndrome (ACS) patients were cultured for 16 hours for the AIM assay with no stimulation or stimulated with P210 peptide or CMV pooled peptides. (A-D) Activation state of PBMCs without peptide stimulation. (E-F) AIM(+) cells in response to P210 or CMV peptide pool. (G-J) PBMCs stimulated with P210 peptide for 72 h and cells were stained for T effector and memory markers. (K) Gating scheme for T effector and memory analysis. Mann-Whitney test except for (C & E), T-test. ‡P=0.07; †P=0.05; *P<0.05. (A-F) Control N=7-8, ACS N=12; some samples/treatments did not have detectable AIM(+) cells so ratio could not be determined. (G-J) Control N=14, ACS N=13.

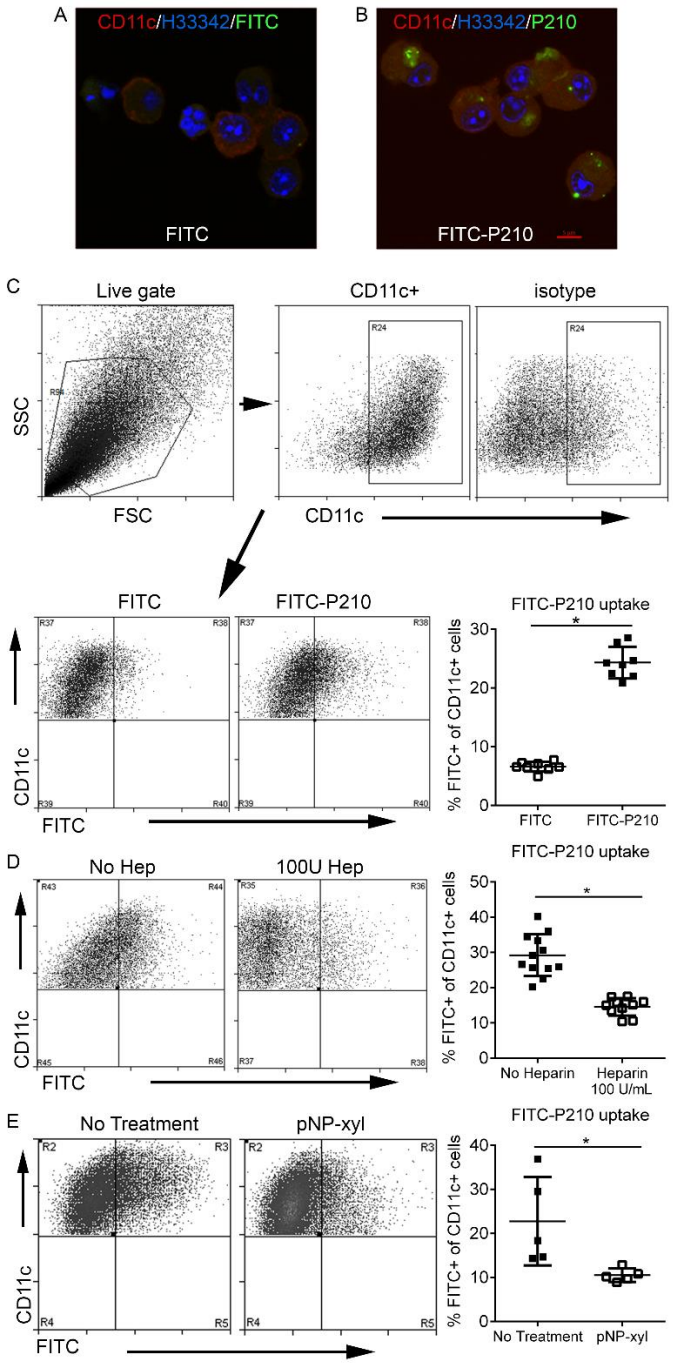

Figure 2: P210-FITC uptake by mouse BMDCs. Confocal microscopy of BMDCs incubated with (A) FITC only or (B) P210-FITC. Same magnification in Fig 2A and 2B and red bar = 5 µm in Fig 2B. (C) FITC internalization was quantified using flow cytometry of CD11c-stained cells. Cells were size gated and then gated on CD11c (C, top panel). $CD11c^+$ cells were then analyzed on CD11c/FITC quadrants and the results plotted on a scatter graph indicating the mean percentage of $FITC^+$ cells on the $CD11c^+$ gate (C, bottom panel; N=8 each). (D) Heparin binds P210-FITC (No heparin N=12; 100U heparin N=10). (E) proteoglycan inhibitor p-Nitrophenyl β-D xylopyranoside (pNP-xyl) blocks proteoglycan-mediated uptake of P210-FITC (N=5 each). *P<0.05, T test.

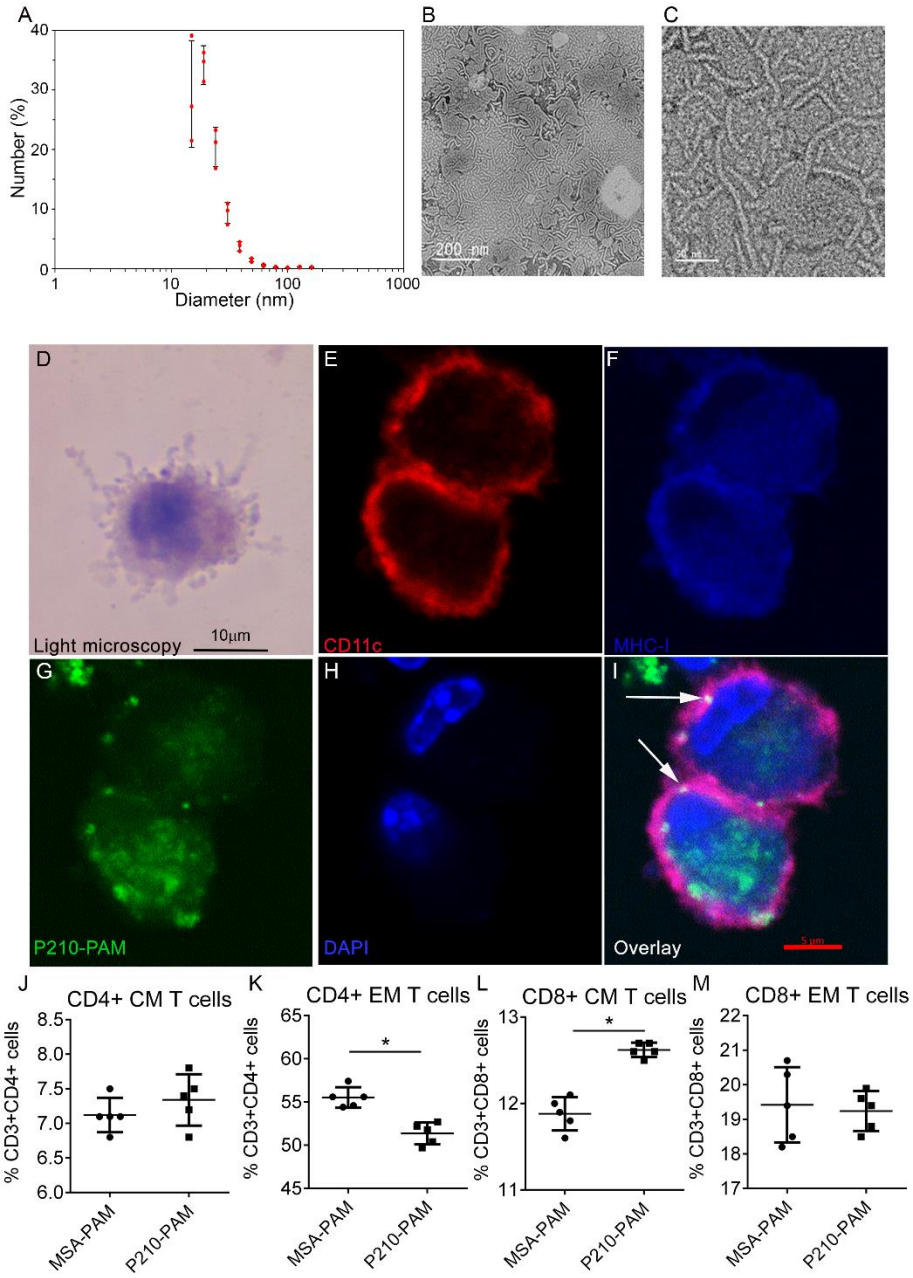

Figure 3: P210-PAM nanoparticles. (A) Majority of P210-PAM are between 15-25 nm in size (N=3). Transmission electron microscopy of P210-PAM at low (B) and high (C) magnification. (D) Light microscopy of Giemsa-stained mouse BMDCs. Fixed BMDCs stained with (E) CD11c PE, (F) MHC-I APC, (G) FITC P210-PAM and (H) DAPI. (I) Color overlay and arrows indicating costaining. The last lysine of the P210 peptide was FITC labeled prior to PAM assembly. Experiment was replicated with similar results. (J) CD4+ central memory (CM) T cells, (K) CD4+ effector memory (EM) T cells, (L) CD8+ CM T cells and (M) CD8+ EM T cells from spleens of 25 weeks old *ApoE*$^{-/-}$ mice fed high fat diet for 16 weeks. Splenocytes were collected after 48h treatment with 20µg/ml MSA-PAM or P210-PAM. N=5 each, $P<0.05$ by T test.

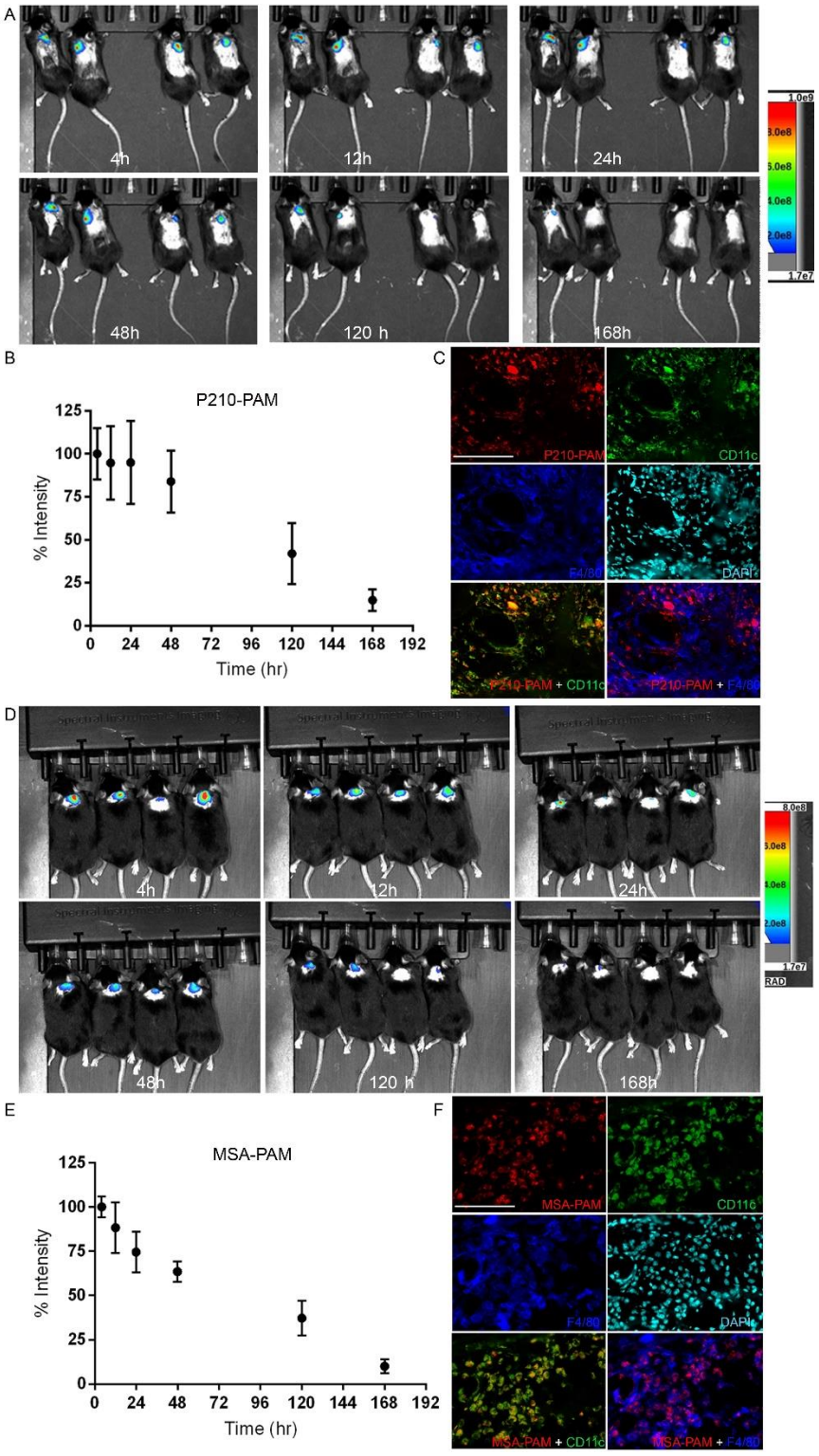

Figure 4: PAM imaging and retention *in vivo*. *In vivo* imaging of P210-PAM (A-C) or MSA-PAM (D-F) retention at injection site of *C57BL/6J* mice over 168h. Percent of signal intensity relative to time zero (immediately after injection) of P210-PAM (B) or MSA-PAM (E). N=4 each. Colocalization of fluorescently labelled P210-PAM (C) or MSA-PAM (F) with F4/80+ macrophages and CD11c+ dendritic cells at the injection site at 48 hours.

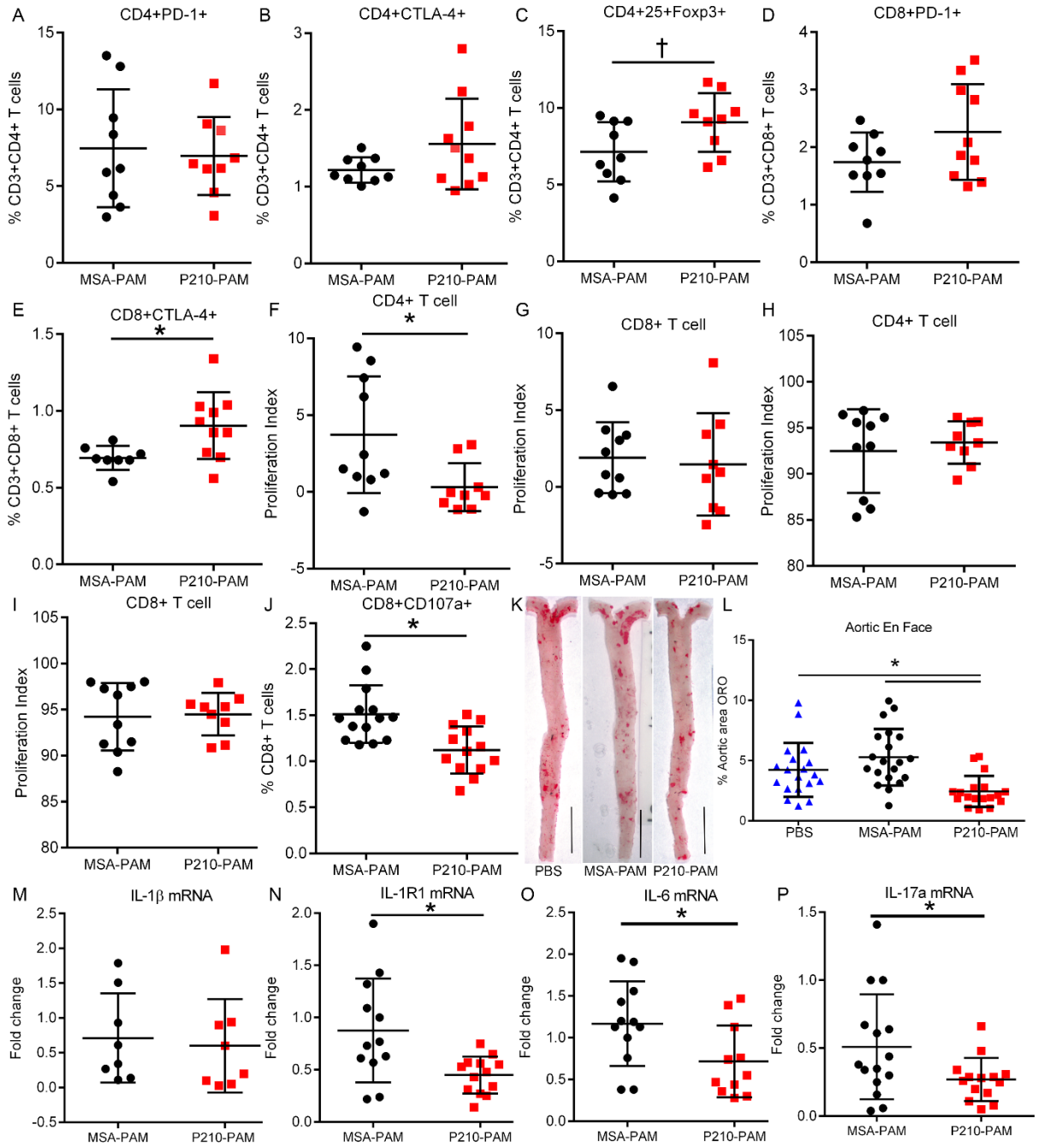

Figure 5: P210-PAM immunization in *ApoE*$^{-/-}$ mice. (A-C) Immune regulatory profile of CD4+ and (D & E) CD8+ T cells in splenocytes of immunized mice 1 week after second booster. (F & G) Splenic T cell proliferation of immunized mice in response to P210 peptide or (H & I) Con A stimulation assessed by BrdU staining. (J) CD107a to assess CD8+ T cell cytolytic activity in splenocytes of immunized mice. (K) Representative photographs of aortic en face staining with Oil red-O at 25 weeks of age. (L) Atherosclerosis measured as percentage of whole aorta stained by Oil red-O. Splenic mRNA expression of (M) IL-1β, (N) IL-1R1, (O) IL-6 and (P) IL-17a. Number of mice used in each group is represented by the number of dots in individual figure. **P*<0.05; †*P*=0.05, T test except for (L) ANOVA with Holm-Sidak multiple comparisons test.

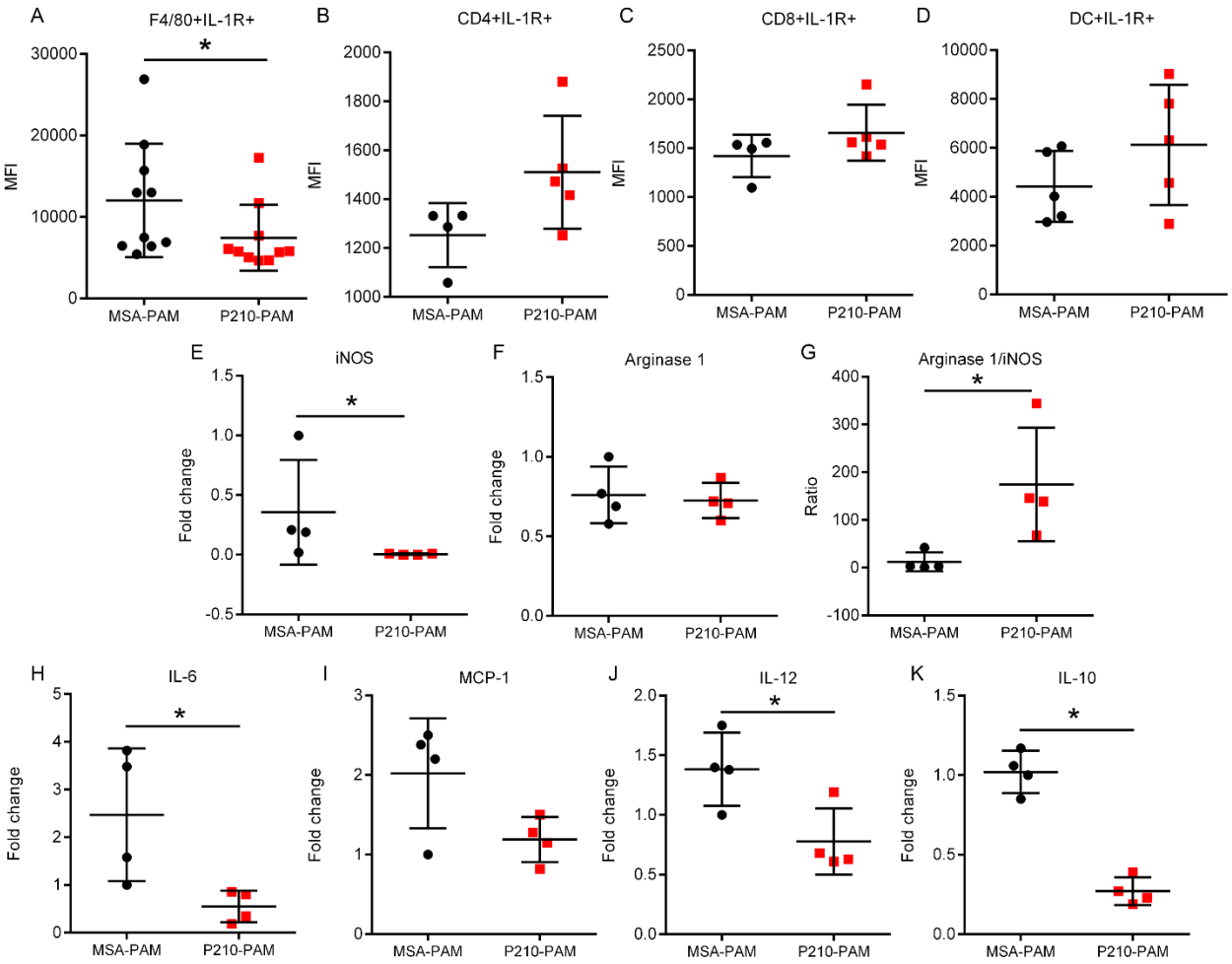

Figure 6: Macrophage phenotype in P210-PAM immunized *ApoE*$^{-/-}$ mice. Splenic IL-1R1 expression measured by MFI in (A) F4/80+ monocyte/macrophage cells, (B) CD4+ T cells, (C) CD8+ T cells, and (D) dendritic cells. Macrophages isolated from peritoneal cavity of immunized mice elicited by thioglycolate injection assessed for (E) iNOS and (F) arginase 1 mRNA expression. (G) Ratio of arginase 1 to iNOS mRNA expression. Macrophages were further phenotyped using mRNA expression of (H) IL-6, (I) MCP-1, (J) IL-12, and (K) IL-10. Number of mice used in each group is represented by the number of dots in individual figure. **P*<0.05 Mann-Whitney for all figures except for (J) and (K) which were analyzed by T test.

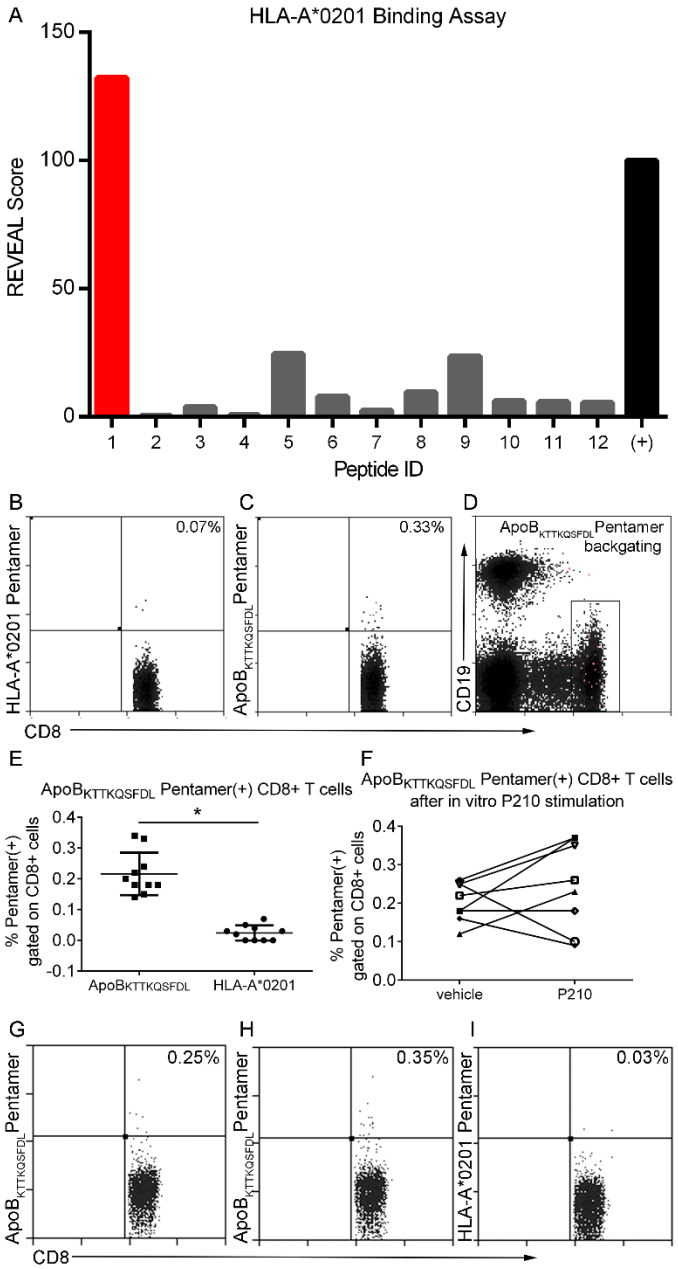

Figure 7: ApoB$_{KTTKQSFDL}$ Pentamer: (A) Binding scores of P210 epitope sequences listed in Table 2 from REVEAL binding assay. Representative plot of PBMCs from HLA-A*02:01(+) volunteer stained with (B) HLA-A*02:01 control pentamer or (C) ApoB$_{KTTKQSFDL}$ pentamer, (D) with backgating in magenta. (E) ApoB$_{KTTKQSFDL}$ pentamer(+) CD8+ T cells in PBMCs of HLA-A*02:01(+) volunteers compared to control HLA-A*02:01 pentamer (N=10). (F) Aliquots available from 8 of the same volunteers were stimulated with 20µg/ml P210 peptide or vehicle (sterile ddH_2O) for 5 days. Representative scatter plot of vehicle (G) or P210 peptide (H) sample stained with ApoB$_{KTTKQSFDL}$ pentamer. (I) The P210 stimulated samples were also stained with HLA-A*02:01 control pentamer as reference for pentamer specificity. *P<0.05 by T test.

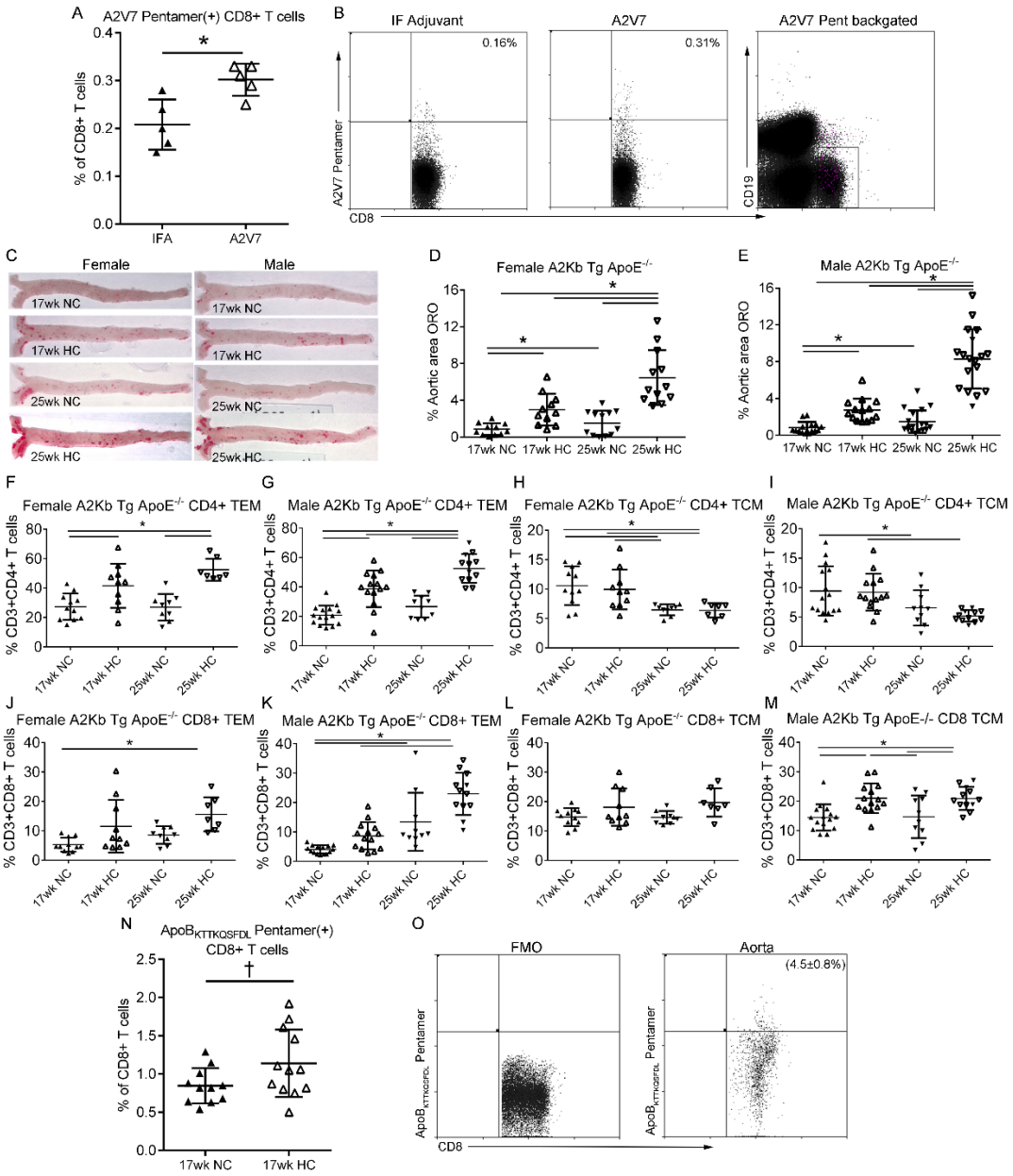

Figure 8: *HLA-A*02:01* transgenic mouse model. (A) Functional test of transgene in *A2Kb Tg ApoE$^{-/-}$* mice immunized with A2V7 and the detection of A2V7 Pentamer(+) CD8+ T cells. (B) Representative scatter plot of A2V7 pentamer(+) CD8+ T cells in adjuvant or A2V7 immunized mice with backgating in magenta. (C) Representative photographs of Oil red-O stained en face aortas from female and male *A2Kb Tg ApoE$^{-/-}$* mice fed normal chow (NC) or high cholesterol diet (HC) for 8 or 16 weeks starting at 9 weeks of age. (D) Aortic atherosclerosis in female and (E) male mice at 17 and 25 weeks of age. (F-I) CD4+ Memory T cells and (J-M) CD8+ Memory T cells in *A2Kb Tg ApoE$^{-/-}$* mice. (N) HLA-A*02:01-P210 pentamer(+) CD8+ T cells in splenocytes of 17-week-old *A2Kb Tg ApoE$^{-/-}$* mice and (O) in plaques of mice aged >63 weeks old after 4 weeks of HC diet feeding; N=4. T test for 2 group comparison; ANOVA with Holm-Sidak multiple comparisons test for more than 2 groups. Number of mice in each group is represented by the number of dots in individual figure. **P*<0.05; †*P*=0.06.

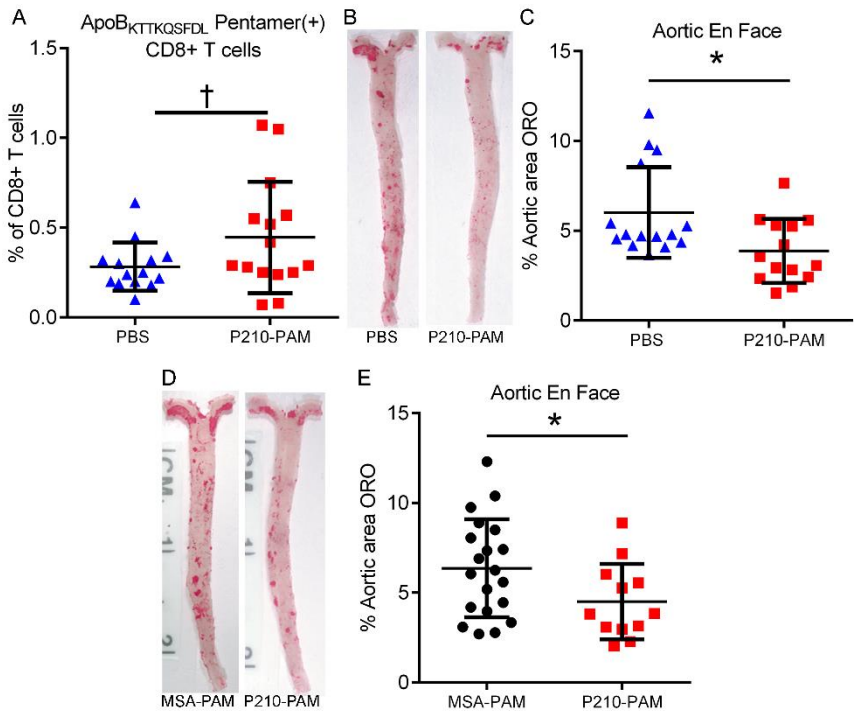

Figure 9: P210-PAM immunized *A2Kb Tg ApoE$^{-/-}$* mice. (A) Detection of ApoB$_{KTTKQSFDL}$ pentamer (+) cells in splenocytes of *A2Kb Tg ApoE$^{-/-}$* mice 13 weeks after second booster injection with either PBS or P210-PAM; †*P*=0.08, T test. (B) Representative photographs of aortic atherosclerosis in these mice. (C) Measurement of percent aortic atherosclerosis area. (D) Representative photographs of aortic atherosclerosis in a second cohort of mice immunized with either MSA-PAM or P210-PAM. (E) Percent aortic atherosclerosis area measurement. *P<0.05, T test.

Figure legends

Figure 1: Intrinsic T cell response to P210 peptide in human PBMCs. Human peripheral blood mononuclear cells from control subjects and acute coronary syndrome (ACS) patients were cultured for 16 hours for the AIM assay with no stimulation or stimulated with P210 peptide or CMV pooled peptides. (A-D) Activation state of PBMCs without peptide stimulation. (E-F) AIM(+) cells in response to P210 or CMV peptide pool. (G-J) PBMCs stimulated with P210 peptide for 72 h and cells were stained for T effector and memory markers. (K) Gating scheme for T effector and memory analysis. Mann-Whitney test except for (C & E), T-test. ‡P=0.07; †P=0.05; *P<0.05. (A-F) Control N=7-8, ACS N=12; some samples/treatments did not have detectable AIM(+) cells so ratio could not be determined. (G-J) Control N=14, ACS N=13.

Figure 2: P210-FITC uptake by mouse BMDCs. Confocal microscopy of BMDCs incubated with (A) FITC only or (B) P210-FITC. Same magnification in Fig 2A and 2B and red bar = 5 μm in Fig 2B. (C) FITC internalization was quantified using flow cytometry of CD11c-stained cells. Cells were size gated and then gated on CD11c (C, top panel). $CD11c^+$ cells were then analyzed on CD11c/FITC quadrants and the results plotted on a scatter graph indicating the mean percentage of $FITC^+$ cells on the $CD11c^+$ gate (C, bottom panel; N=8 each). (D) Heparin binds P210-FITC (No heparin N=12; 100U heparin N=10). (E) proteoglycan inhibitor p-Nitrophenyl β-D xylopyranoside (pNP-xyl) blocks proteoglycan-mediated uptake of P210-FITC (N=5 each). *P<0.05, T test.

Figure 3: P210-PAM nanoparticles. (A) Majority of P210-PAM are between 15-25 nm in size (N=3). Transmission electron microscopy of P210-PAM at low (B) and high (C) magnification. (D) Light microscopy of Giemsa-stained mouse BMDCs. Fixed BMDCs stained with (E) CD11c PE, (F)

MHC-I APC, (G) FITC P210-PAM and (H) DAPI. (I) Color overlay and arrows indicating costaining. The last lysine of the P210 peptide was FITC labeled prior to PAM assembly. Experiment was replicated with similar results. (J) CD4+ central memory (CM) T cells, (K) CD4+ effector memory (EM) T cells, (L) CD8+ CM T cells and (M) CD8+ EM T cells from spleens of 25 weeks old *ApoE*$^{-/-}$ mice fed high fat diet for 16 weeks. Splenocytes were collected after 48h treatment with 20µg/ml MSA-PAM or P210-PAM. N=5 each, $P<0.05$ by T test.

Figure 4: PAM imaging and retention *in vivo*. *In vivo* imaging of P210-PAM (A-C) or MSA-PAM (D-F) retention at injection site of *C57BL/6J* mice over 168h. Percent of signal intensity relative to time zero (immediately after injection) of P210-PAM (B) or MSA-PAM (E). N=4 each. Colocalization of fluorescently labelled P210-PAM (C) or MSA-PAM (F) with F4/80+ macrophages and CD11c+ dendritic cells at the injection site at 48 hours.

Figure 5: P210-PAM immunization in *ApoE*$^{-/-}$ mice. (A-C) Immune regulatory profile of CD4+ and (D & E) CD8+ T cells in splenocytes of immunized mice 1 week after second booster. (F & G) Splenic T cell proliferation of immunized mice in response to P210 peptide or (H & I) Con A stimulation assessed by BrdU staining. (J) CD107a to assess CD8+ T cell cytolytic activity in splenocytes of immunized mice. (K) Representative photographs of aortic en face staining with Oil red-O at 25 weeks of age. (L) Atherosclerosis measured as percentage of whole aorta stained by Oil red-O. Splenic mRNA expression of (M) IL-1β, (N) IL-1R1, (O) IL-6 and (P) IL-17a. Number of mice used in each group is represented by the number of dots in individual figure. *$P<0.05$; †$P=0.05$, T test except for (L) ANOVA with Holm-Sidak multiple comparisons test.

Figure 6: Macrophage phenotype in P210-PAM immunized *ApoE*$^{-/-}$ mice. Splenic IL-1R1 expression measured by MFI in (A) F4/80+ monocyte/macrophage cells, (B) CD4+ T cells, (C)

CD8+ T cells, and (D) dendritic cells. Macrophages isolated from peritoneal cavity of immunized mice elicited by thioglycolate injection assessed for (E) iNOS and (F) arginase 1 mRNA expression. (G) Ratio of arginase 1 to iNOS mRNA expression. Macrophages were further phenotyped using mRNA expression of (H) IL-6, (I) MCP-1, (J) IL-12, and (K) IL-10. Number of mice used in each group is represented by the number of dots in individual figure. *P<0.05 Mann-Whitney for all figures except for (J) and (K) which were analyzed by T test.

Figure 7: $ApoB_{KTTKQSFDL}$ Pentamer: (A) Binding scores of P210 epitope sequences listed in Table 2 from REVEAL binding assay. Representative plot of PBMCs from HLA-A*02:01(+) volunteer stained with (B) HLA-A*02:01 control pentamer or (C) $ApoB_{KTTKQSFDL}$ pentamer, (D) with backgating in magenta. (E) $ApoB_{KTTKQSFDL}$ pentamer(+) CD8+ T cells in PBMCs of HLA-A*02:01(+) volunteers compared to control HLA-A*02:01 pentamer (N=10). (F) Aliquots available from 8 of the same volunteers were stimulated with 20µg/ml P210 peptide or vehicle (sterile ddH_2O) for 5 days. Representative scatter plot of vehicle (G) or P210 peptide (H) sample stained with $ApoB_{KTTKQSFDL}$ pentamer. (I) The P210 stimulated samples were also stained with HLA-A*02:01 control pentamer as reference for pentamer specificity. *P<0.05 by T test.

Figure 8: *HLA-A*02:01* transgenic mouse model. (A) Functional test of transgene in *A2Kb Tg ApoE*$^{-/-}$ mice immunized with A2V7 and the detection of A2V7 Pentamer(+) CD8+ T cells. (B) Representative scatter plot of A2V7 pentamer(+) CD8+ T cells in adjuvant or A2V7 immunized mice with backgating in magenta. (C) Representative photographs of Oil red-O stained en face aortas from female and male *A2Kb Tg ApoE*$^{-/-}$ mice fed normal chow (NC) or high cholesterol diet (HC) for 8 or 16 weeks starting at 9 weeks of age. (D) Aortic atherosclerosis in female and (E) male mice at 17 and 25 weeks of age. (F-I) CD4+ Memory T cells and (J-M) CD8+ Memory T

cells in *A2Kb Tg ApoE*$^{-/-}$ mice. (N) HLA-A*02:01-P210 pentamer(+) CD8+ T cells in splenocytes of 17-week-old *A2Kb Tg ApoE*$^{-/-}$ mice and (O) in plaques of mice aged >63 weeks old after 4 weeks of HC diet feeding; N=4. T test for 2 group comparison; ANOVA with Holm-Sidak multiple comparisons test for more than 2 groups. Number of mice in each group is represented by the number of dots in individual figure. *P<0.05; †P=0.06.

Figure 9: P210-PAM immunized *A2Kb Tg ApoE*$^{-/-}$ mice. (A) Detection of $ApoB_{KTTKQSFDL}$ pentamer (+) cells in splenocytes of *A2Kb Tg ApoE*$^{-/-}$ mice 13 weeks after second booster injection with either PBS or P210-PAM; †P=0.08, T test. (B) Representative photographs of aortic atherosclerosis in these mice. (C) Measurement of percent aortic atherosclerosis area. (D) Representative photographs of aortic atherosclerosis in a second cohort of mice immunized with either MSA-PAM or P210-PAM. (E) Percent aortic atherosclerosis area measurement. *P<0.05, T test.

Table 1: Characteristics of human subjects.

	Control (N=14)	**ACS (N=13)**
Mean age	58.2±10.4	58.1±14.6
Male sex	71%	77%
Mean LDL cholesterol (mg/dL)	N/A	109.6±40.3
Use of cholesterol lowering medication*	N/A	46%

ACS: acute coronary syndrome; N/A: not available; *determined at time of admission, 1 patient was on Praluent.

Table 2: P210 epitope analysis.

Peptide ID	Sequence
1	KTTKQSFDL*
2	TTKQSFDLS
3	TKQSFDLSV
4	KQSFDLSVK
5	QSFDLSVKA
6	SFDLSVKAQ
7	FDLSVKAQY
8	DLSVKAQYK
9	LSVKAQYKK
10	SVKAQYKKN
11	VKAQYKKNK
12	KAQYKKNKH

Sequential 9-mer P210 peptides analyzed for binding to HLA-A*02:01. *High binding score as depicted in corresponding REVEAL binding assay result in Figure 7A.